NON-LETHAL FOAM DEPLOYMENT SYSTEM FOR VEHICLE STOPPING

by

MATTHEW E SCHROEDER

B.S., Kansas State University, 2008

A THESIS

submitted in partial fulfillment of the requirements for the degree

MASTER OF SCIENCE

Department of Chemical Engineering
College of Engineering

KANSAS STATE UNIVERSITY
Manhattan, Kansas

2010

Approved by:

Major Professor
Dr. Glasgow

Abstract

The military is interested in stopping suspicious vehicles at checkpoints or security positions while minimizing noncombatant fatalities. Preliminary work has shown that decreasing the oxygen concentration in proximity to the automobile air intake system and blocking the air flow through an automotive induction system provides the greatest probability of success for the broadest possible array of internal combustion engines.

A non-lethal foam deployment system was developed that satisfies the military's needs to stop suspicious vehicles. The foam is discharged from a pressurized tank and engulfs the air intake system of the target vehicle. The foam is drawn into the air intake and the protein additive contained in the foam would occlude pores in the air filter medium. Once the air filter was blocked, the vehicle would become immobilized so that security personnel can secure the vehicle.

The work carried out in this project consisted of development and refinement of surfactant solution composition, improvement in the rate of absorption of carbon dioxide for increased foam volume, and characterization of discharge for optimum foam volume. In addition, a half-scale model apparatus was developed to test the foam's ability to be ingested in an automotive intake system. These experiments demonstrated that the foam deployment system would stop an automobile within six seconds.

Table of Contents

List of Figures

List of Tables

Acknowledgments

The work and information shared in this THESIS is only possible through the support of others. For this, a special thank you to the College of Engineering at Kansas State University, the Chemical Engineering department and most importantly the sponsoring Professor, Dr. Glasgow. Dr Glasgow spent many hours providing the guidance and recommendations during the final preparation of the Thesis. I would also like to thank my friend, Lance Williamson for his help on this project and the many questions he was able to answer. I am grateful for my parents Stan and Rosanne Schroeder for their support during the process of my graduate program. They kept me motivated and encouraged me to finish my thesis. Finally, these acknowledgments would not be complete without thanking everyone who either advised me or helped edit the many rough drafts of this paper. Lastly, I want to thank M2 technologies for financial support that made this project a success.

Preface

The development of non-lethal systems for protecting the interests and assets of the United States of America has assumed new urgency. One area of particular concern is that the United States military minimizes civilian casualties in theaters of operation where insurgents employ nontraditional methods and weapons (e.g., improvised explosive devices). The concern over civilian casualties has led to the development of precision ordinances and non-lethal systems to minimize noncombatant fatalities. The research and development of such systems are a military and political priority.

This research at Kansas State University focused upon how to disable suspicious vehicles without injuring the occupants. During past heightened security situations, concrete barriers were strategically deployed to control vehicular traffic around government buildings and military establishments. In the present work, security measures were developed which focused on a non-lethal foam deployment system for vehicle stopping. The foam is discharged from a pressurized tank and engulfs the air intake system of the target vehicle. The foam is drawn into the air intake, and the protein additive contained in the foam occludes pores in the air filter medium. Once the air filter was blocked, the vehicle becomes immobilized so that security personnel could secure the vehicle. Research on surfactant composition and foam properties will be presented in the following chapters.

CHAPTER 1 - Introduction

The use of foams in modern society is pervasive. There are many industrial applications including fire suppression, soaps, insulation, and personal care products. The evolution of foams has progressed from fermented beverages to advanced oil recovery. The following chapter is a history and literature review regarding pertinent aspects of foam. The history review documents the evolution of foam, while the literature review will focus upon the foam's composition. The history and literature review provide a starting point for the development of the rapid engine suffocant.

History

Foams can be described by an array of definitions that distinguish the fine line between liquid and gas phases. Foam is defined by dictionary.com as "a mass of small bubbles formed in or on a liquid," or "a substance that is formed by trapping many gas bubbles in a liquid or solid." Adamson and Gast (1997) noted in Physical Chemistry of Surfaces that foams are defined as "two partially miscible fluids and, usually, a surfactant." To further distinguish between foams and emulsions, they state, "if both phases are liquid, the system is called an emulsion, whereas if one fluid is a gas, the system may constitute a foam or an aerosol." The difference between an aerosol and foam is that an aerosol is comprised of more gas than liquid, while a foam consists of more liquid than gas. The definitions can be combined and result in "foam" being defined as a gas entrapped in a liquid phase. A solid phase entrapping a gas phase can also constitute foam, but this type of foam will not be considered in this study.

Liquid foam can be categorized as either transient (wet) or stable (dry), and each type can be used to advantage for specific industrial applications. Typical foam applications include carbonated beverages, spray insulation, fire suppression, liquid extraction, mineral separation, and improved oil recovery. The one that is nearest in relevance for the intent of this project is fire suppression foam.

The main goal of fire suppression foam is to eliminate a fire, and there are several ways in which this can be accomplished. A fire can be stopped by removing the combustible material or by preventing oxygen from reaching the fire. Blocking the transport of oxygen is generally

easier then eliminating a fuel source and usually less dangerous. For this purpose, dry and wet foams have been developed for fire suppression. The original fire extinguishers produced acidic foam from sodium bicarbonate and glacial acetic acid. Additional fire suppression systems were developed using trichlorcarbonate solution, but these materials were later found to be hazardous because of the chlorides (History of the Antique Fire Extinguisher, 1972). Fire suppression systems continue to evolve because of the advent of jet fuels and high voltage lines; this evolution was documented and published in "Fire-Fighting Foams and Foam Systems", 1972. The research led to the development of the fluorinated haloalkane surfactant suppression system in 1964, which improved the way fires were fought by replacing solid-based fire extinguishers that were used solely for petroleum-based fires (National Fire Protection Association, 1972).

Not only have fire suppression foams evolved, but other products such as oil enhancement foams, carbon sequestration foams, and mineral suppression foams have been developed. Oil enhancement foams were created to be stable in hydrocarbon environments (such as underground oil reservoirs), but still have transient characteristics that allow for fluid motion in an oil well. Carbon sequestration foams were developed with an affinity for carbon dioxide over other carbon-based materials. Separation of solid and liquid phases can be improved with foams because of foam's ability to entrain solid particles. These current industrial applications of foam can be used as guides for development of the initial composition of the surfactant solution.

Literature Review

Foam Composition

The composition of the surfactant solution is an important aspect for the production of foams in this project. The review of current research allowed for an initial surfactant composition to be determined and indicated how this composition would affect foam characteristics. The following literature review covers foam composition and foam expansion.

Foam Fluidity

There are two types of foams that can be generated: transient (wet) and stable (dry). Transient foams are characterized by their ability to flow, while stable foams have limited drainage over time. Both of these properties can increase the potential and effectiveness for the

intended application. There are four standard foam tests used to characterize a particular foam as either a transient or stable foam and the results can be used to optimize the foam composition.

The transient behavior of foam can be studied by measuring the rate at which the foam flows in a pipe. One such experiment is called the "Briceno and Joseph" test. The apparatus for this test consists of a vessel filled with surfactant solution. Air is passed through the surfactant solution and is mixed to produce foam. The foam flows through a piping system which contains four pressure sensors used to determine the change in pressure as the foam traverses the pipe. An illustration of the apparatus can be seen in Figure 1.1 (Briceno and Joseph, 2003).

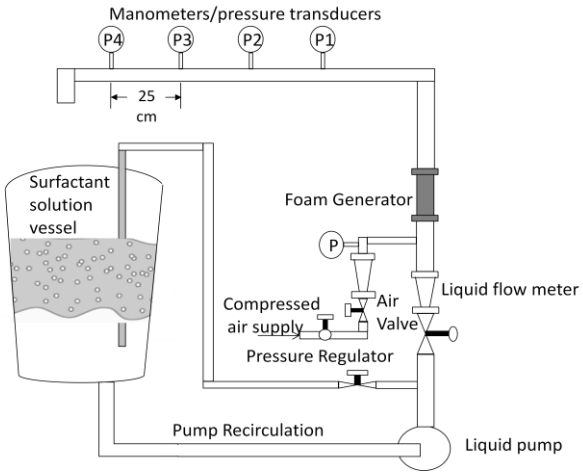

Figure 1.1: "Briceno and Josepeh" apparatus for determining the transient behavior of foam.

The "Briceno and Joseph" test measures the fluidity of the foam at various qualities. The quality of the foam is determined by the ratio of the volumetric flow rate of air to the total volumetric flow rate of both the surfactant and air through the system. Once the flow rates are set the foam flows through the duct system and pressure can be measured as the foam travels through the duct. This measurement of quality of foam versus the pressure is used to compare fluidity of foam composition trials. A sample result of the experiment is figure 1.2.

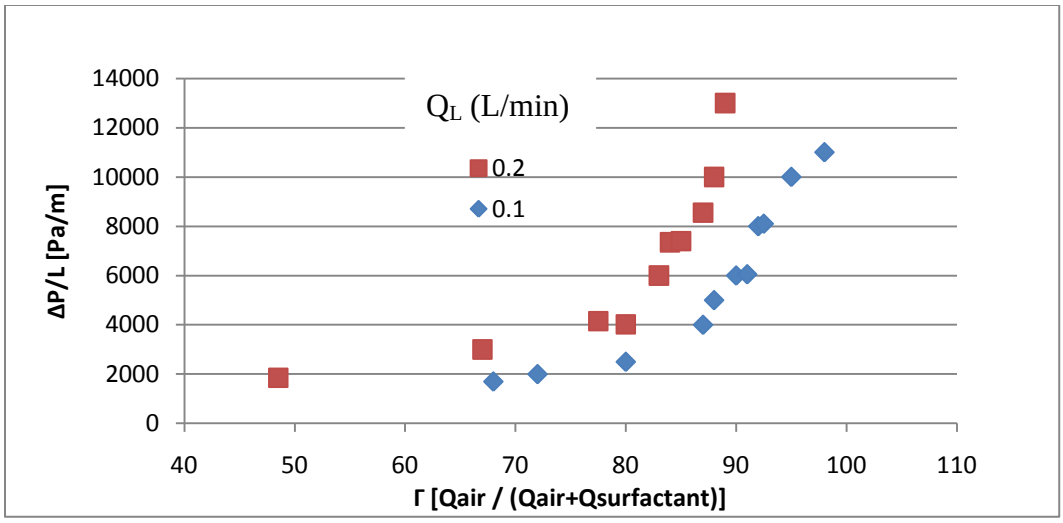

Figure 1.2: Adapted sample results of "Briceno and Josepeh" test for anionic surfactant (sodium dodecyl sulphate) and 1-butanol.

The figure represents an adapted sample result of an anionic surfactant and 1-butanol (Briceno and Joseph, 2003). The figure shows that increasing the air in the surfactant solution will increase the fluidity of the foam. The "Briceno and Joseph" test needs to be conducted during the surfactant composition trials to compare each composition and find the optimal fluidity.

Foam stability is considered a key variable that relates to both the persistence of the foam and the liquid drainage. There are three experiments (similar to the "Briceno and Joseph" test) commonly used to characterize the stability of foam. The first experiment, called "Ross-Miles" test, is completed by measuring a specific volume of foam and placing it in a column. The foam will then degrade with time and measurements can then be taken on the rate of degradation by volume (Jonsson, Lindman, Holmberg, and Kronberg, 1998). The second stability test requires a vessel be filled with a surfactant solution. Then 100 ml of air flows through the solution, and the maximum amount of foam generated is measured by volume. The change in volume with time is measured to determine the stability of the foam (Lunkenheimer and Malysa, 2003). The third test is the "Bikerman Method," and it is completed by filling a tube with the solution and having a air flow through it. There will be a rise in the volume of foam that can be measured. The air is then turned off and the decay of the foam is measured by volume (Jonsson, Lindman, Holmberg, and Kronberg, 1998). The results of the three experiments can be used to compare surfactant composition, and determine the most stable foam that is produced.

A combination of fluidity and stability test can be used to characterize the surfactant solution composition. However, the foam's characteristics can be enhanced through optimization of the surfactant solution composition. To increase the transient behavior of the foam, water or an additional surfactant is added. The stability of foams can be improved by avoiding oils and adding viscosifers to the surfactant solution (Gautam and Mohanty, 2004). Experimentation on the composition of the surfactant solution was completed and will be presented in future chapters.

Foam Volume

For the project to be a success, a large quantity of foam must be generated quickly. Several approaches for increasing the foam volume were reviewed, including increasing the concentration of surfactant solutions, decreasing the concentration of oils, adding protein or other solids to the solutions, and adding viscosifers to the solution. Increasing the surfactant concentration can increase the amount of foam that can be generated, while hydrocarbons decrease the stability of the foam. Adding proteins or solid particles (such as polymers) allows for increased interaction between the liquid and solid phases. This increased interaction results in a greater entrapment of gas in a liquid. Another method of increasing the volume of the foam is to increase the viscosity of the surfactant solution. Increasing the viscosity can be done by adding viscosifers, such as xanthum gum or guar gum to the solution. The amount of viscosifers must be accurately measured because too much could result in the foam being very stable with limited fluidity, and too little will result in fluid foam that lacks stability (Gautam and Mohanty, 2004).

To predict foam volume, several models have been developed to explain foam interactions and expansion of foam during discharge. Each model was initially developed by assuming that foams behave as a granular mixture. One particular model, the discrete element method (DEM), is a numerical method that analyzes the foam at the bubble level and assumes that each bubble is independent. The DEM model attempts to track or predict the movement of each bubble in the mixture. This model works well for small applications, but the required computation power is too great when trying to track every bubble in a very large system and other models should be used. These techniques include high resolution homogenization schemes or micromechanical models. The high resolution homogenization scheme assumes each bubble is identical in nature, and each phase is homogenous. However, this model does not track each bubble or each bubble's characteristics. The micromechanical model, with the assumption that

each bubble has uniform radius, works for a pure bubble solution but the solution is a multiphase solution and not pure bubbles. To counter the problems with the two models, a combination of models must be used. For example, the combination of the homogenization scheme and a micromechanical model would counter the flaws, and a reasonable model could be developed. The results of the model would predict what is happening on the surface of the foam. The DEM and micromechanical models were presented in detail in "The Link Between Discrete and Continuous Modeling of Liquid Foam at the Level of a Single Bubble" (Gardiner and Tordesillas, 2005).

Conclusion

It was found that the quality of the foam can be improved by changing the composition of the surfactant solution. Increasing the water concentration improves the transient behavior, while increasing the viscosifer concentration consequently makes the foam more stable. Oil adversely affects the foam volume, while viscosifers and surfactants produce more foam. A combination of models, the homogenization scheme and the micromechanical model, can then be developed to understand how the foam will behave during deployment and usage. Surfactant solution composition experiments were developed based on the literature review, the data of which will be presented in future chapters.

CHAPTER 2 - Foam Composition and Optimization

Introduction

The objective of this project is the development of a stand-off system of minimum lethality, which is capable of stopping an approaching automobile or light truck and rendering it inoperable for at least 10 minutes. The previously conducted review by Dr. Glasgow of this scenario revealed five options:

- Decreasing the oxygen concentration in proximity to the intake
- Blocking the air flow through the induction system
- Interrupting the fuel flow to the engine
- Changing the fuel properties (alter volatility, viscosity, flammability)
- Disrupting the electrical system so that the fuel-air mixture cannot be ignited (not applicable to diesel vehicles).

Preliminary work has shown that a combination of the first two options provides the greatest probability of success for the broadest possible array of internal combustion engines.

One of the methods offering the highest probability of success is a foam spray material. The foam spray would be discharged at an automobile and then engulf the air intake system. The foam can either be developed by a chemical reaction (such as sodium bicarbonate and acetic acid) or from a pressurized cylinder that is filled with a surfactant solution that is saturated with carbon dioxide. Both methods for foam production were considered in this work.

Either of the two methods for producing foam must result in an adequate volume being developed and a feasible deployment. The chemical reaction method required mixing the contents of two independent tanks to produce foam; however, two tanks are logistically impractical for this application. On the other hand, a surfactant solution partially saturated with carbon dioxide can be premixed and contained in a single tank. Therefore, surfactant based foams are considered more portable and practical for this application. However, the composition of the foam solution must be optimized for the desired rapid expansion, transient behavior, and the stability enhanced.

Foam Composition

The composition of the surfactant solution must result in a foam being developed that satisfies the requirements of this project. To determine the foam's characteristics, several experiments had to be conducted on foam volume, foam stability, and foam enhancement (to improve air filer pore occlusion). Before these experiments were completed, preliminary work determined that a suitable candidate solution might consist of water, sodium lauryl sulfate, cocamide diethylamine (DEA), and egg protein.

Foam Volume

The volume of the foam that can be generated is the single most important characteristic. The volume of foam was tested and the experiments were designed to systematically test three independent variables. The following table shows the results of the experiments, with the total foam volume and the composition of the solution.

Table 2.1: Trial recipes

Water (mL)	Sodium Lauryl Sulfate (mL)	Cocamide DEA (mL)	Egg Protein (g)	Total Surfactant Volume (mL)	Foam Volume (L)
4440	560	115	24	5075	15
4440	560	140	24	5100	24
4440	560	210	0	5170	30
4440	535	210	26	5200	32
4440	535	210	78	5200	34

The procedure for making the surfactant solution is as follows:

1) Measure each ingredient
2) Mix the water with the egg protein
    - The mixture will be yellow in color
3) Add the sodium lauryrl sulfate and cocamide DEA

- The final solution with have a high viscosity and will be saturated with air bubbles

4) Put the solution into an aluminum (beverage) cylinder and allow it to rest for 24 hrs
5) Then pressurize the cylinder with 800 psi carbon dioxide and let it rest for 10 to 12 hrs
    - The carbon dioxide will diffuse into the solution over time
6) Repeat the pressurization process approximately 7-10 times (100-120 grams of carbon dioxide will absorb)
    - Once the head space pressure remains at 800 psi after 12 hrs the solution is ready for release.
7) Open all valves and release the surfactant solution to produce foam

This was the initial experimental procedure used for the small-scale testing of foam volume. Improvements to this process are discussed in Chapter 3: Absorption of Carbon Dioxide. Even though the process was later improved, important information was collected from these early experiments. For example, it was found that increasing the concentration of cocamide DEA (115 to 210 ml) resulted in an increased foam volume. The other factor that affected foam volume was the concentration of surfactant that was added to the solution. The experiments of foam were conducted on surfactant and cocamide DEA concentration (presented in Table 2.1), but it was determined that the absorption of carbon dioxide had a greater impact on foam volume. The egg protein seemed to have very little effect on the final foam volume, but the particles suspended in solution were required to occlude the air filter.

Stability

The stability of the foam is crucial to development of a feasible product. The stability was measured by bubble size distribution and observing foam degradation over time. The foam's characteristics can be enhanced by using these experimental results and changing the foam composition.

The bubble size distribution experiment was developed to assess the stability of the foam at the bubble (microscopic) level. An experimental apparatus was constructed with a Plexiglas^{tm} box, sponge, four washers, and a Plexiglas^{TM} plate. A sponge was placed on top of the box and water flows over the sponge. A laminar flow regime develops and foam is slowly poured onto

the water. The water then forces the foam under a Plexiglas™ plate that is raised with four washers. The water is turned off and a mono bubble layer is formed. The single bubble layer is back-lighted to enable a digital image of the layer to be taken. Images were recorded every minute for 30 minutes and each image subsequently analyzed using commercial software (Sigma Scan Pro 5). The following figure is a picture of the bubble imaging apparatus.

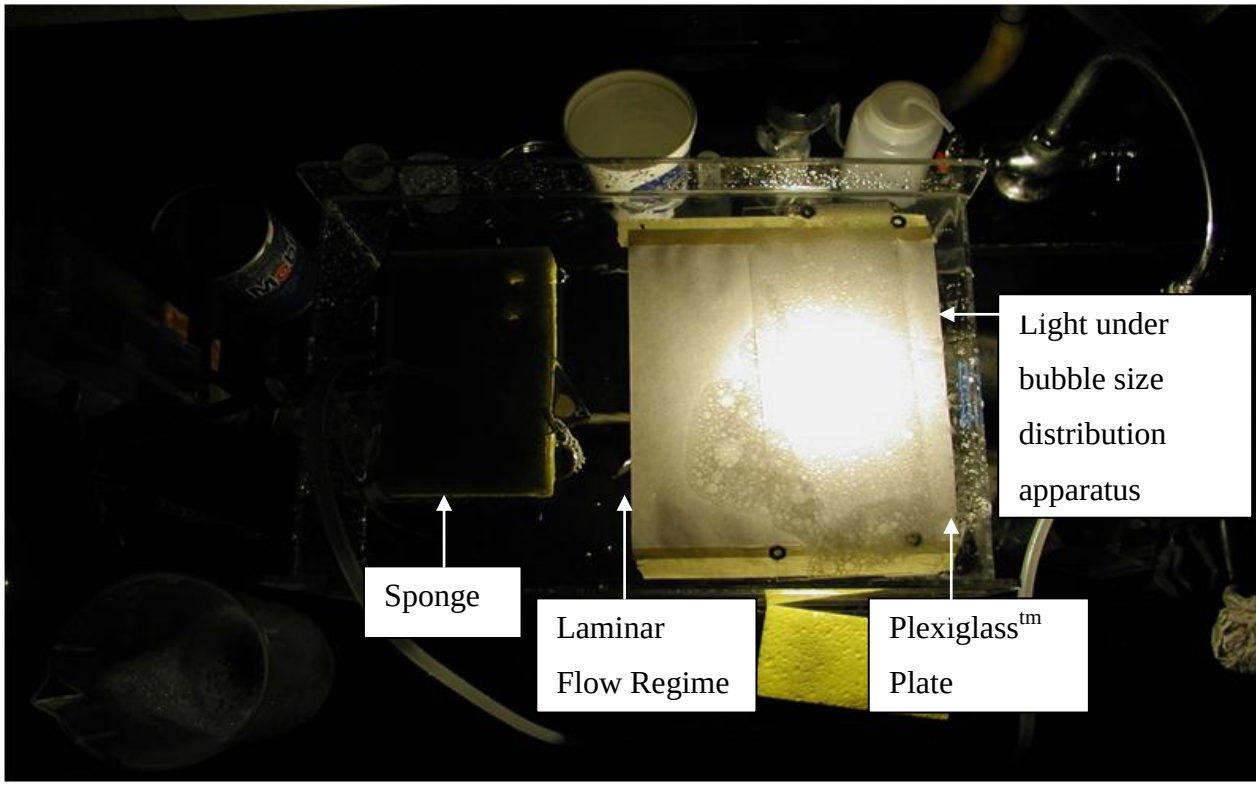

Figure 2.1: Photograph of the bubble image apparatus used to take pictures of a back lighted foam mono layer.

The following procedure was used to measure the bubble distribution:

1) Set up the apparatus and wet the sponge.
2) Flow water over the top of the sponge at a low flow rate.
    - The water forms a laminar flow regime on the surface of the Plexiglas™ container.
3) Collect the foam spray and slowly pour it onto the water.
4) Once the foam forms a monolayer under the Plexiglas™ plate, the water is turned off.
5) Photographs are then taken of the monolayer of foam every minute for 30 minutes.

6) The images are then converted to black and white and analyzed using Sigma Scan Pro 5 software.
7) A bubble size distribution can be then formed with multiple images.

The bubble size distribution reveals the breakage and the stability of the foam. The following images show the raw bubble size data at t=0 and t=30 minutes.

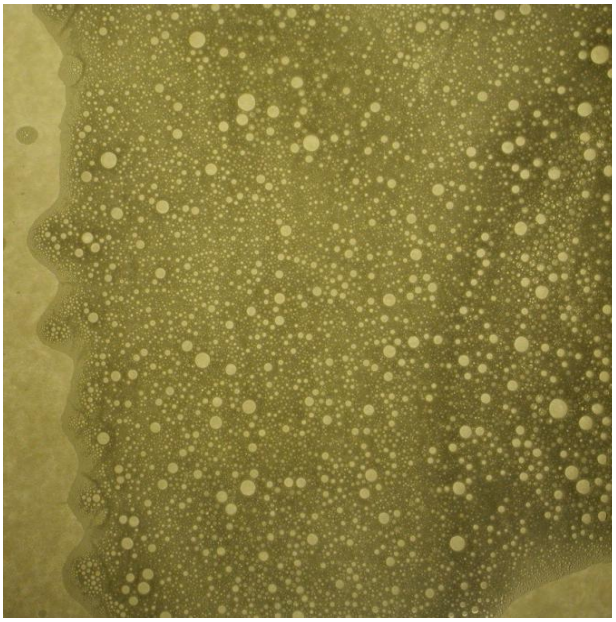

Figure 2.2: Image for bubble size measurement in foam layer at t=0.

Figure 2.3: Image for bubble size measurement in foam layer at t=30 minutes.

A comparison of the two images shows a decrease in both bubble size and volume of foam after 30 minutes. This resulted from foam drainage and breakage of the larger bubbles. An image analysis using Sigma Scan Pro 5 was performed on each of the images taken from the bubble size distribution experiment. A sample of the analysis, figure 2.4, depicts the distribution of bubble sizes at t=0, 15, and 30 minutes.

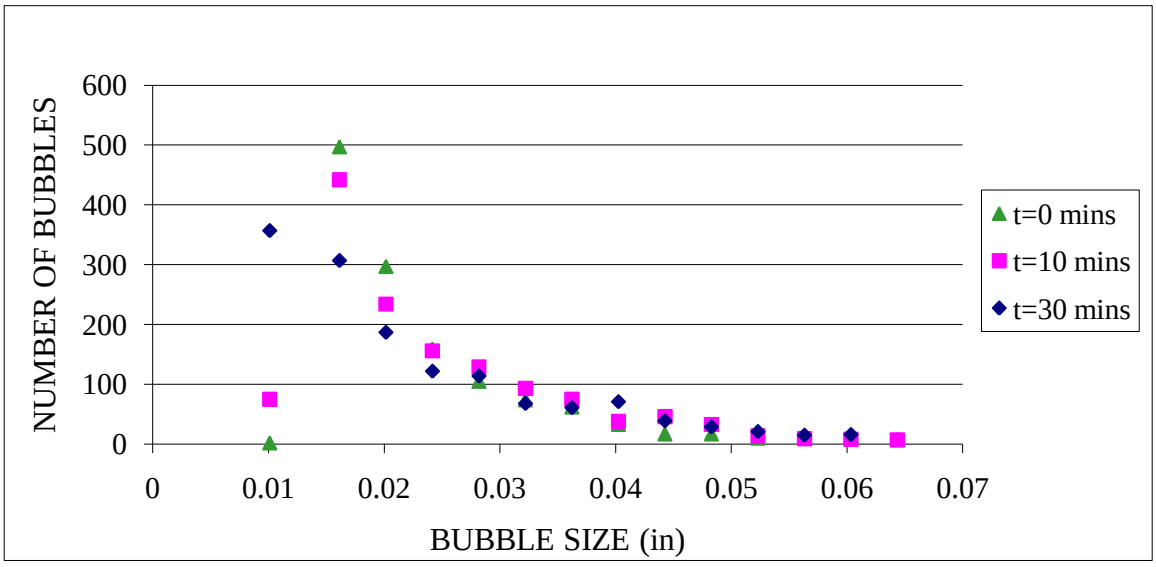

Figure 2.4: Bubble size distribution at t=0, 10, and 30 minutes for the bubble images of Figures 2.2 and 2.3.

The bubble size distribution has the shape $f(x) = 1/\beta\ e\text{^}(-x/\beta)$ where β is a constant between 0 and 1. The bubble size distributions indicate that over time, the average bubble size decreases, but the decay rate of the bubbles is very slow. The slow decay rate is an indicator of foam stability and will allow substantial time for the target vehicle to be disabled.

The bubble size distribution is crucial for quantifying foam degradation with time. The decay of the bubble with time will determine the stability of the foam and the suitability of the foam for the intended application. These experiments showed that in a lab environment, the foam will persist for at least 30 minutes, but different ambient conditions could decrease the stability of the foam.

Foam Enhancement for Occluding Air Filter Media

Foam, enhanced with egg protein, was tested on an automotive air filter. These experiments analyzed a filter before and after the exposure of foam provided both direct visualization and pressure results. In addition, these experiments determined if the particles can block the air flow in an automobile air intake system.

The filter characterization apparatus consists of an automotive air filter, foam, pressure transducer, Hirsch funnel, aspirator, and vacuum flask. An air filter is placed inside a Hirsch funnel, and the funnel is placed on top of the vacuum flask. A vacuum flask is connected to a vacuum gauge and an aspirator. Foam is collected and placed inside the Hirsch funnel. A vacuum is applied to the funnel, and the foam is drawn through the filter. After the foam has been applied to the flask, the suction continues until no air flow can penetrate the filter, resulting in a dramatic drop in pressure. Digitized video stills at about 400X are taken of the filter before and after the trial for visual verification of the filter pore occlusion. Figures 2.5 and 2.6 are digitized video stills of the filter paper surface at about 400X.

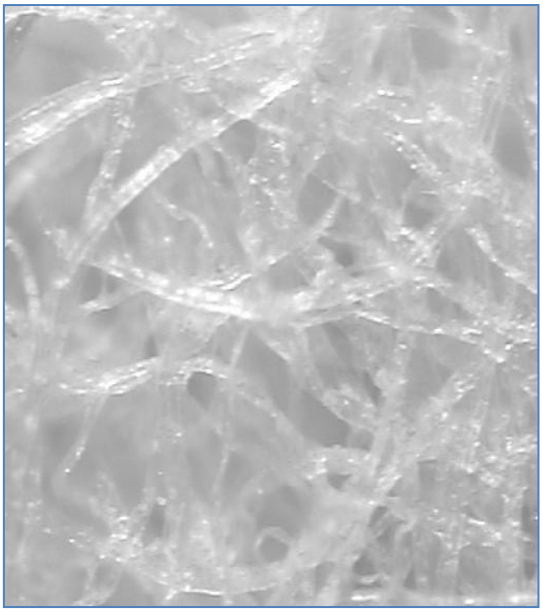

Figure 2.5: Surface of filter medium before contact with foam

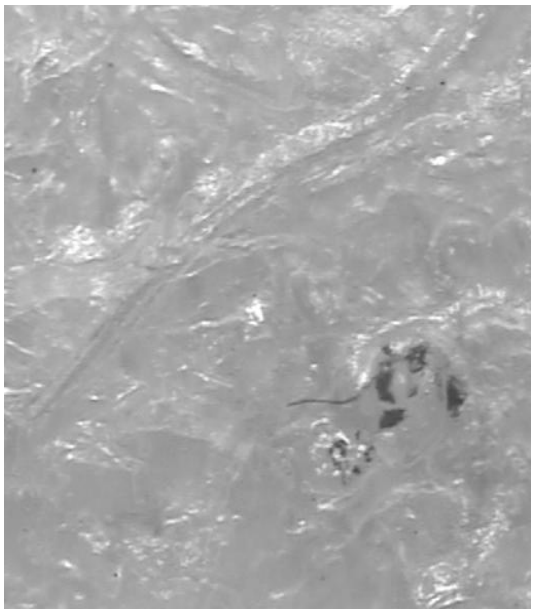

Figure 2.6: Surface of filter medium after contact with foam

Figure 2.5 is a digitized video still of filter medium before foam has been applied. The image shows individual strands of the paper medium that allow foreign particulate matter to be collected during normal operations. Figure 2.6 is the same filter after the foam was drawn through the filter medium. One can see the outline of the filter paper mesh, but no distinct pores can be determined from the image. These images show how the protein enriched foam occludes the filter medium and prevents air from passing through. To determine the time it takes to occlude the filter, a pressure transducer was used and the response to the vacuum can be seen in Figure 2.7.

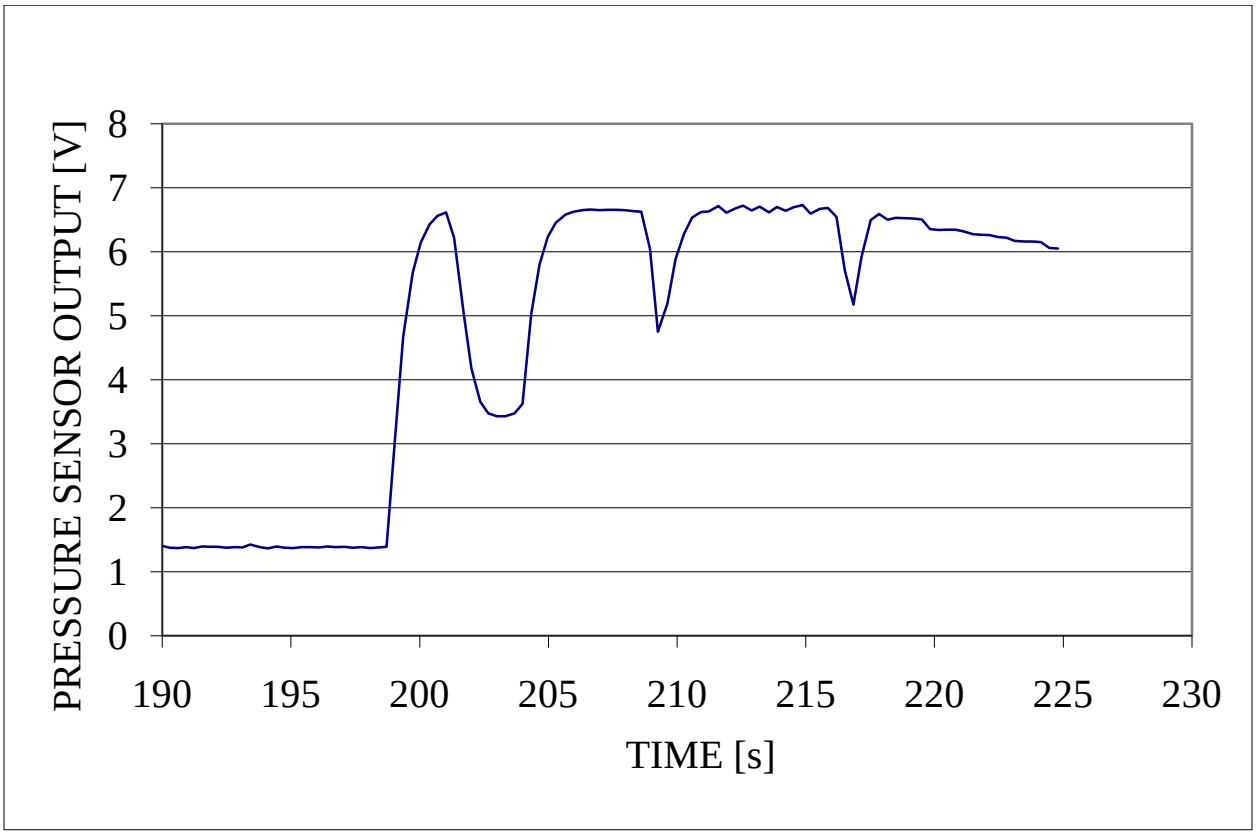

Figure 2.7: Pressure record during the process of clogging a filter

The foam was applied to the filter at 198 seconds and flow through the filter was blocked in about two seconds according to the Figure 2.7. The figure also shows that at t=204, 210, and 215 seconds there were drops in output voltage of the pressure sensor. The spikes in voltage were directly related to a decrease in the vacuum pressure. This drop in vacuum pressure was caused by foam bypassing the filter on the outside edge of the filter medium. The occluding of the filter results in an automobile shutting down, and without replacement of the filter it will not start.

Foam System Scale Up

Although the foam successfully occluded pores in the filter media in repeated small-scale experiments, the question still arises regarding the ease with which the foam will enter the air intake system. To increase the chances of success of foam ingestion, large quantities of foam will be required to engulf the air intake system. Therefore, a test was performed on increasing the

volume of the foam, to determine the viability. The scale-up process required doubling the initial volume of the initial surfactant solution and adding Xanthum gum to the solution. Viscosifers, such as xanthum gum, affect both the stability and flow of the foam. The following is the composition of the surfactant solution after large scale trials were completed with xanthum gum.

Water (mL)	Sodium Laryrl Sulfate (mL)	Cocamide Dea (mL)	Xanthum Gum (g)	Egg Protein (g)	Total Foam Volume (L)
8800	1070	420	100	144	65

The improved procedure for larger-scale foam test is as follows:

1) Measure each ingredient
2) Mix part of the water with xanthum gum until the solid is dissolved
    - The mixture will be grey in color and have a very high viscosity
3) Mix the rest of the water with the egg protein
    - The mixture will be yellow in color
4) Mix the two solutions together
5) Add the sodium lauryrl sulfate and cocamide DEA
    - The final solution with have a high viscosity, (roughly 525 cp) and will be saturated with air bubbles
6) Put the solution into an aluminum (beverage) cylinder and allow it to rest for 24 hrs
7) Then pressurize the cylinder with 800 psi carbon dioxide and let it rest for 10 to 12 hrs
    - The carbon dioxide will diffuse into the solution over time
8) Repeat the pressurization process approximately 7-10 times (100-120 grams of carbon dioxide will absorb)
    - Once the head space pressure remains at 800 psi after 12 hrs the solution is ready for release.
9) Open all valves and release the surfactant solution to produce foam

The final foam volume varied from trial to trial but it was roughly 10 to 15 times the surfactant solution volume. This increase in final volume was related to both the emulsifier and the total volume of carbon dioxide that could be absorbed. While the small scale surfactant trials had a liquid to foam ratio of about 1/5. With the addition of xanthum gum and increased concentration of carbon dioxide the foam generation increased by 10 to 15 times.

Conclusion

The foam composition (for enhanced properties) was developed for a non-lethal system that will stop an automobile remotely. Improving the surfactant solution was one of the major goals of this project. The surfactant solution composition was tested, but additional research should be conducted on concentration of cocamide DEA and sodium laryrl sulfate to increase the volume of foam.

CHAPTER 3 - Carbon Dioxide Absorption

The main objective of this project, as described in Chapter 2, was to provide a non-lethal system that can be used to stop suspicious automobiles approaching check points or other military installations. Preliminary work by Dr. Glasgow has shown that decreasing the oxygen concentration in proximity to the intake by blocking the air flow through the induction system would provide the greatest probability of success for the broadest possible array of internal combustion engines. To engulf the intake system of an automobile, large quantities of foam must be generated either from a chemical reaction or from a surfactant solution that is saturated with carbon dioxide. Producing the foam by chemical reaction was deemed impractical for logistical reasons, while producing foam (from a pressurized surfactant solution) was determined to be viable for this application. When the solution is released to the atmosphere, dissolution of carbon dioxide will result in foam being produced. To enhance and increase the foam volume that can be generated, the amount of carbon dioxide that is absorbed into the surfactant solution must be maximized/optimized.

The absorption of carbon dioxide into the surfactant solution is affected by the chemical interaction between the pertinent species. This interaction is governed by thermodynamics (enthalpy, surface tension, and the Gibbs energy) of a multiphase solution (Rocha and Johnston, 2000). To improve the multiphase behavior additional chemical components can be added to the surfactant solution.

One chemical species that can be added to the solution is diethylamide, which has an affinity for carbon dioxide at elevated pressure. While diethylamide has been commonly used to improve carbon dioxide loading, additions of alkanolamine solutions can produce better results than diethylamides (Kundu and Bandyopadhyay, 2006). The alkosolution that was recommended was diethanolamine (DEA) (Kundu and Bandyopadhyay, 2006). This addition resulted in an improved absorption of the carbon dioxide into the solution. The improved absorption was a result of more favorable interaction of the carbon dioxide with the amines in the solution. Another possible addition to the amine solutions presented is ferrofluids to increase the absorption rate of carbon dioxide. The problem with ferrofluids is the environmental concern, therefore they were not considered for further use in this study (Komati and Akkihebbal, 2008). A major component that affects the absorption of carbon dioxide is surfactants. The addition of

surfactant to the solutions would improve the rate of absorption of carbon dioxide, the equilibrium concentration of carbon dioxide was not affected by adding surfactants to the solution (Farajzadeh, Barati, Delil, and Bruining, 2007; Wei-rong, Hui-xiang, & Da-hui, 2004). The addition of the surfactant solution is an important step in the production of foam, and additional research on the chemical interaction should be studied.

The amount of carbon dioxide that can be absorbed by the surfactant solution is, of course, governed by its solubility. The solubility of carbon dioxide in water has been studied by U.S. Department of Energy (U.S Department of Energy) and Kansas Geological Survey (Carbon Dioxide Solubility in Water, 2003). Figure 3.1 is the experimental result of the concentration of carbon dioxide with respect to temperature and it shows that an increased temperature of the solution results in a decreased solubility of carbon dioxide (Engineeringtoolbox.com, 2005). This decreased absorption of carbon dioxide adversely affects the ability to generate foam. The pressure also influences the amount of carbon dioxide that can be absorbed by aqueous solution. Figure 3.2 illustrates the solubility of carbon dioxide based on pressure at temperature ranging from 70 to 130ºF (Carbon Dioxide Solubility in Water, 2003). The concentration of carbon dioxide in water increases substantially from 0 to 900 psi, but after 900 psi the increase slows. The diminishing increase in solubility with increasing pressure is the main reason the cylinder is only being pressurized to 800 psi.

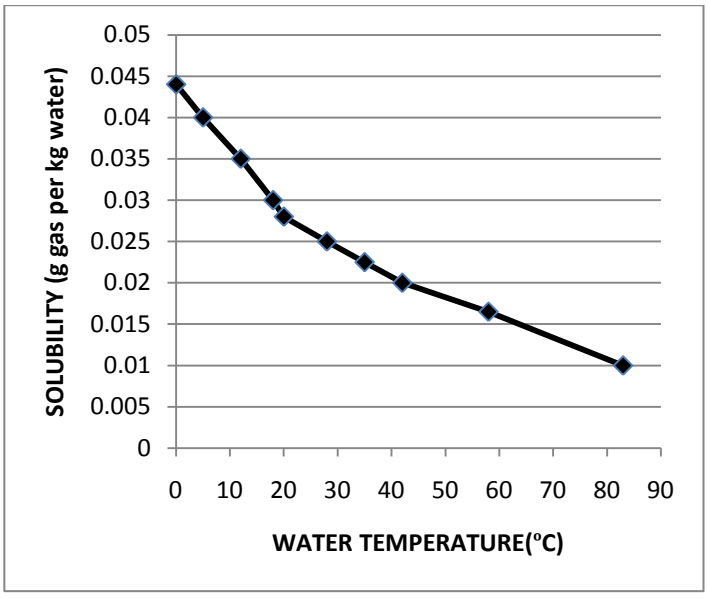

Figure 3.1: Carbon dioxide solubility in aqueous media with respect to temperature at a constant pressure of one atmosphere, adapted from Engineeringtoolbox.com plot.

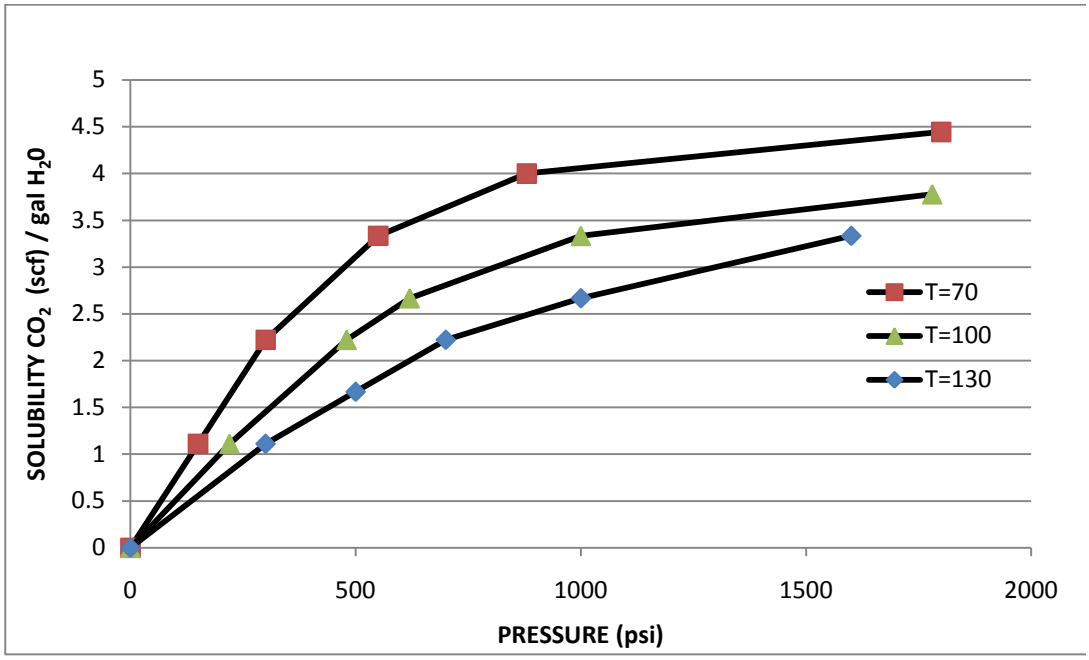

Figure 3.2: Solubility of carbon dioxide with respect to pressure at T= 70, 100, 130 ºF, extrapolated from the Kansas Geological Survey plot.

There are two primary methods for the absorption of carbon dioxide into surfactant solution: diffusion in a stationary fluid and diffusion that is enhanced by fluid motion. Both methods require a specialized apparatus consisting of an aluminum (beverage) cylinder 61 cm tall and 18 cm in diameter. The cylinder has a total volume of 13.52 liters, and the surfactant solution occupied 10.8 liters. This gives a head space of 2.72 liters. The vessel is pressure rated to 1000 psi, but the cylinder is only pressurized to 800 psi. The two techniques have different rates of absorption and to better understand what was happening in the solution, each system was modeled. These two techniques will be explained, and the models for the techniques will be discussed in detail.

Diffusion Model for Vertical Orientation

The transport of carbon dioxide into a surfactant solution can be modeled to determine the rate of absorption, as well as the depth of penetration of the carbon dioxide into the surfactant solution. The model is diffusion dependent and contains only one constant. This constant is the diffusivity coefficient for the absorption of carbon dioxide into the surfactant solution, and it must be determined before the model can be used. The experimental system described by this

model involves a motionless, vertical cylinder as depicted in figure 3.3. The diffusion of the gas only occurs at the free surface, which is the cross section of the tank (πR^2). In Figure 3.3 a diagram of the absorption of carbon dioxide inside a vertical fixed oriented cylinder is illustrated. The governing equation for molecular diffusion of carbon dioxide into the liquid in the cylinder is:

$$\frac{\partial x_A}{\partial t} = \frac{\partial}{\partial y}\left(D \frac{\partial x_A}{\partial y}\right) \qquad 3.1$$

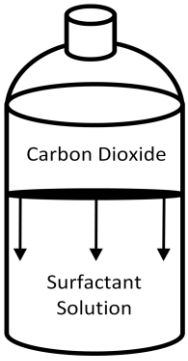

Figure 3.3: Cylinder diagram in a fixed vertical orientation.

The left side of equation (3.1) accounts for the accumulation of carbon dioxide. The right hand side of the equation (3.1) is molecular (diffusional) transport in the y-direction. x_A is mole fraction of carbon dioxide in the liquid phase, y is the vertical direction, and D is the diffusivity. Initially, the concentration of carbon dioxide at the surfactant solution interface is zero. Upon contact, the interfacial equilibrium composition is established rapidly, and the tank is considered semi-infinite such that there is no solute far from the interface. To solve the parabolic partial differential equation (PPDE) analytically, a scaling transformation is applied to the equation. A new independent variable is defined as $\eta = \frac{y}{\sqrt{4D_{AB}\, t}}$, and introduced into (3.1) The transformation of the PPDE produces an ordinary differential equation that has a standard solution, equation (3.2).

$$\frac{x_A}{x_{Ao}} = 1 - \text{erf}\left(\frac{y}{\sqrt{4D_{AB}t}}\right) \qquad 3.2$$

The analytical solution can be used to determine the extent to which the carbon dioxide would penetrate the surfactant solution and the time required for the absorption of carbon dioxide.

The fixed orientation model was used to estimate the rate of absorption of carbon dioxide for the diffusion-limited method in a fixed cylinder, and it demonstrated that the time required to

achieve saturation would be impractically long. The model predicted that the total concentration and penetration depth of the carbon dioxide into the solution, as well as the time required for the absorption process. These results are presented in Figures 3.4 and 3.5.

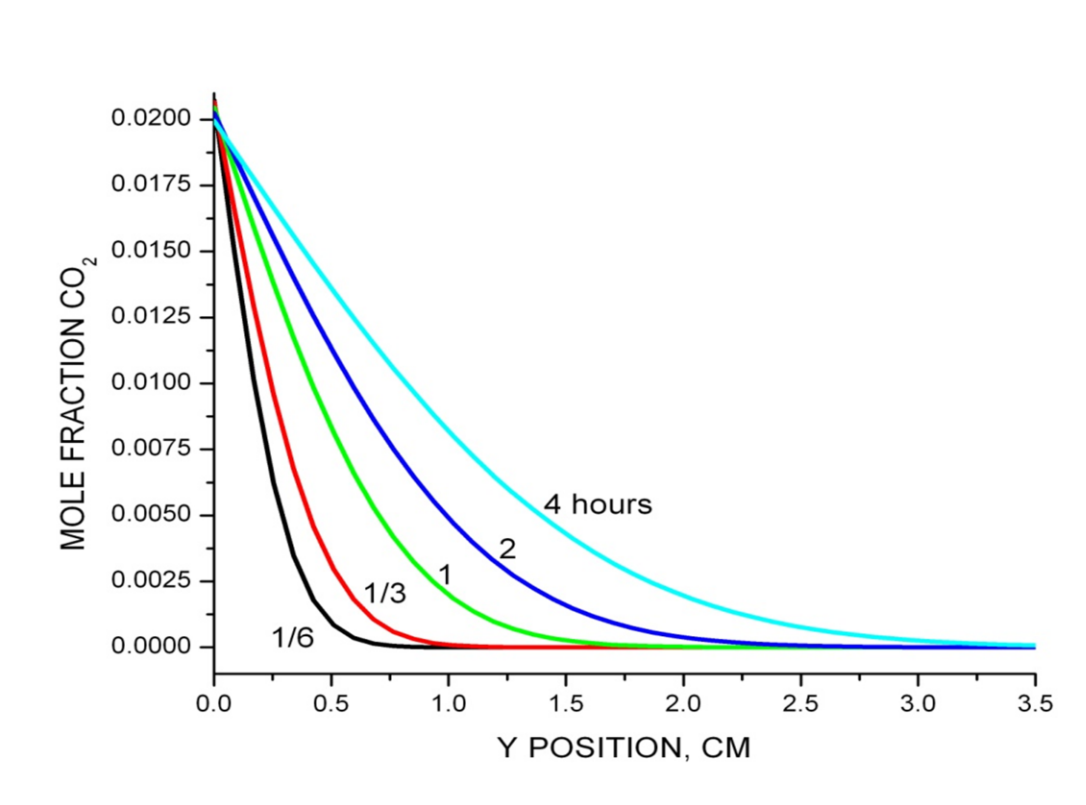

Figure 3.4: Diffusional transport model results for the carbon dioxide absorption and penetration into the liquid phase with increasing time.

Figure 3.4 illustrates the concentration of carbon dioxide as a function of both time and penetration into the surfactant solution. The figure demonstrates that that carbon dioxide would only effectively penetrate about 3 cm into the surfactant solution in 4 hours. In Figure 3.5 another result of the model is presented, and it is the head space pressure as a function of time.

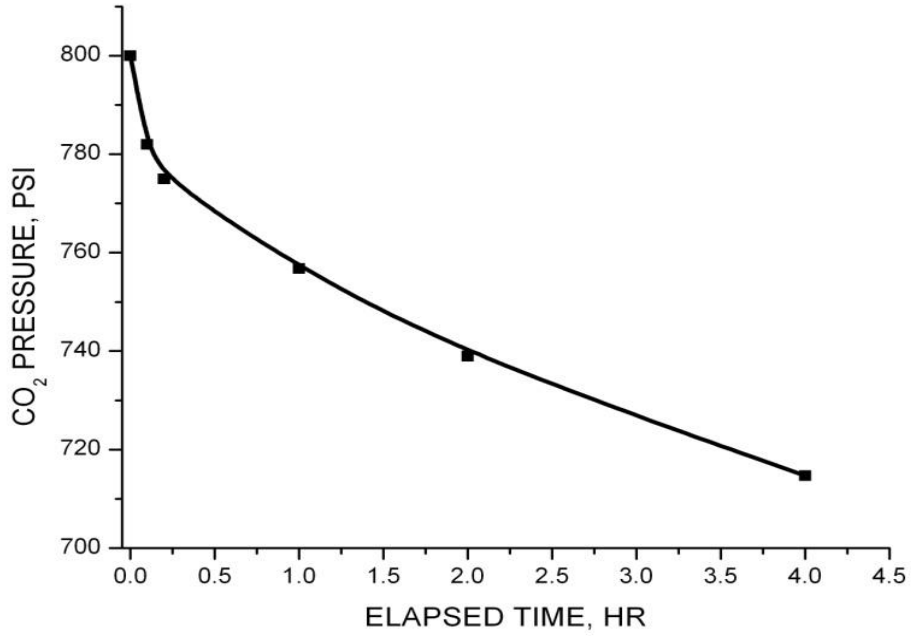

Figure 3.5: Head space pressure in the cylinder over four hours of the absorption process.

The above figure shows computed results from the model for the head space pressure inside the cylinder. The calculation shows that the head space pressure decreases rapidly in the first 30 minutes and then the rate of change decrease dramatically, suggesting that carbon dioxide absorption slows with time. The model was extrapolated to determine the diffusion-limited mass transfer time, and it was determined that after 7-8 hours the change in pressure is very small. This suggests that the cylinder should be repressurized every 7-8 hours to allow for optimum absorption of carbon dioxide. The experimentation will be discussed in detail in the following section.

Experimental Diffusion of Carbon Dioxide into a Vertical Cylinder

To produce foam, the cylinder containing the surfactant solution had to be charged with carbon dioxide. To prepare a cylinder, surfactant solution is made and poured into the cylinder. The head space of the cylinder is then filled with 800 psi carbon dioxide. The cylinder is allowed to sit in a vertical orientation, and the carbon dioxide diffuses into the solution. The cylinder is

recharged periodically, and the pressure is monitored over time to determine the amount of carbon dioxide that was absorbed by the solution.

The experimental trials were completed and measurements of the head space pressure in the cylinder were recorded. The pressure record, Figure 3.6, presents detailed information on the absorption process.

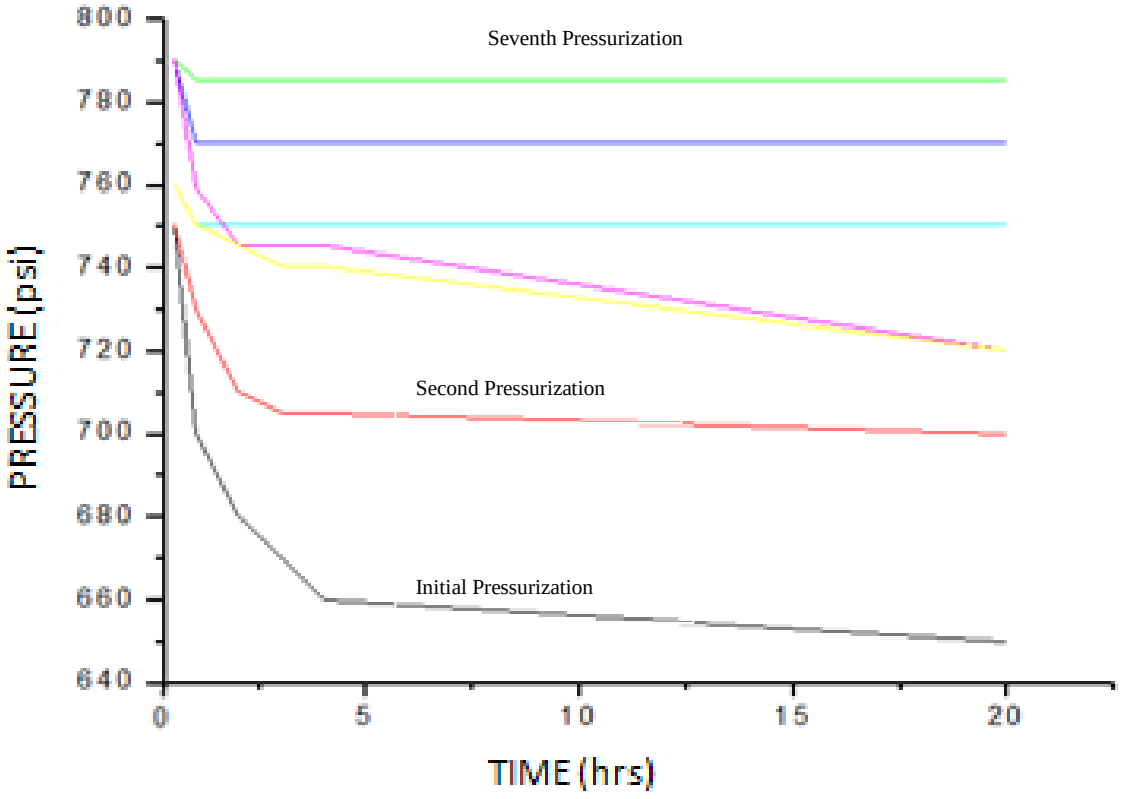

The above figure illustrates the absorption process over seven pressurization cycles. The results from the experiments confirmed that the absorption process is very slow and requires days to partially saturate the solution.

The change in pressure needs to be converted to moles to determine the amount of carbon dioxide that was absorbed by the solution. To convert the pressure to moles the ideal gas law, equation 3.3, was used, although the generalized compressibility factor indicates some deviation from ideality.

$$PV = nRT \qquad 3.3$$

P is the pressure of the head space of the container, V is the volume of the head space, 2.72 liters, n is the number of moles in the gas phase, R is the gas constant, and T is the temperature of the room which is assumed constant at 25 º C. The change in pressure of the head space allowed for the total number of moles absorbed to be calculated. From the number of moles the mass of carbon dioxide that was absorbed can be calculated. With diffusion-limited absorption, the surfactant solution absorbed a total of 116.55 grams of carbon dioxide over seven repeated pressurizations. The highest rate of absorption occurred at the initial charging, but over time the rate of absorption decreased dramatically. This decrease in the absorption of carbon dioxide occurred in the experiment and was fully expected because of the results of the diffusion-limited model.

The diffusion-limited absorption experiments resulted in carbon dioxide being absorbed too slowly by the surfactant solution; this is completely impractical for the intended application. A different technique was required to improve the rate of absorption of carbon dioxide and hasten the approach to saturation. A method for the enhanced absorption of carbon dioxide was developed that used fluid motion (convective transport) to increase the rate of mass transfer.

Mass transfer for a Rotating Cylinder

The diffusion-limited method of carbon dioxide absorption proved to be inadequate as it resulted in a surfactant solution that was only partially saturated. It became clear that fluid motion would be required to accelerate the absorption process. There were three alternatives considered, each subject to the requirements that the device must be simple to build, improve the rate of absorption, and limit the amount of heating due to viscous dissipation. The alternatives included rolling the tank in a horizontal fashion (similar to a ball mill), using an oscillating motion (similar to a paint can shaker), or rotating the cylinder end-over-end (similar to a drum mixer). Each of the concepts posed problems, and solutions were sought prior to actual development. The rolling of the cylinder posed a safety hazard if the tank was not properly controlled. Rapid and vigorous oscillations would generate heat due to viscous dissipation and adversely affect the absorption of carbon dioxide. Finally, rotating the cylinder end-over-end

posed too many mechanical difficulties. It was determined that rolling the cylinder in a horizontal fashion was the easiest method for enhancing molecular diffusion with fluid motion.

Modeling Mass Transfer for the Rotating Tank

The rotation of the tank greatly increased the rate at which the carbon dioxide could be absorbed into the surfactant solution. Naturally, the increased amount of carbon dioxide absorbed improved the quality of foam. To better understand what was happening during the absorption process, a model of the convective transport process was developed.

The velocity distribution of the liquid in the rotating cylinder was developed using two-components of the Navier-Stokes equation in cylindrical coordinates (r and θ), assuming viscous forces are dominant. The resulting velocity distribution was then used with the continuity equation to model solute transport.

$$\frac{\partial^2 v_r}{\partial r^2} + \frac{1}{r}\frac{\partial v_r}{\partial r} - \frac{v_r}{r^2} + \frac{1}{r^2}\frac{\partial^2 v_r}{\partial \theta^2} - \frac{2}{r^2}\frac{\partial v_r}{\partial \theta} \cong 0 \qquad 3.4$$

$$\frac{\partial^2 v_\theta}{\partial r^2} + \frac{\partial}{\partial r}\left(\frac{v_\theta}{r}\right) + \frac{1}{r^2}\frac{\partial^2 v_\theta}{\partial \theta^2} - \frac{2}{r^2}\frac{\partial v_\theta}{\partial \theta} \cong 0 \qquad 3.5$$

These equations describe viscous transport of momentum in the radial and angular directions. These two equations model the flow field of the rotating surfactant solution inside the cylinder but the absorption process is modeled by equation (3.6), the continuity equation.

$$\frac{\partial C}{\partial t} + v_r\frac{\partial C}{\partial r} + \frac{v_\theta}{r}\frac{\partial C}{\partial \theta} = D\left[\frac{\partial^2 C}{\partial r^2} + \frac{1}{r}\frac{\partial C}{\partial r} + \frac{1}{r^2}\frac{\partial^2 C}{\partial \theta^2}\right] \qquad 3.6$$

This equation uses the principle of conservation of mass to determine how the solute (carbon dioxide) is distributed throughout the aqueous surfactant solution. To develop the model for absorption, two experiments (flow visualization and viscosity determination) were required before the three equations could be solved simultaneously.

The velocity profile is determined by equations (3.4) and (3.5) and is subject to both a Dirichlet and Neumann type boundary condition. The Dirichlet boundary condition states the velocity of the fluid at the wall is equal to the velocity of the cylinder due to the no slip condition boundary condition. The Neumann type boundary condition states that there is no momentum flux across the gas-liquid interface. A numerical solution, using the boundary conditions, can be used to approximate the fluid velocity. To substantiate the model's predictions, a flow visualization experiment was conducted.

To provide verification for the velocity distribution, a flow visualization experiment was conducted. The model cylinder was built using a PVC pipe and Plexiglas^{TM} caps that allow visualization (and imaging) of the fluid motion.

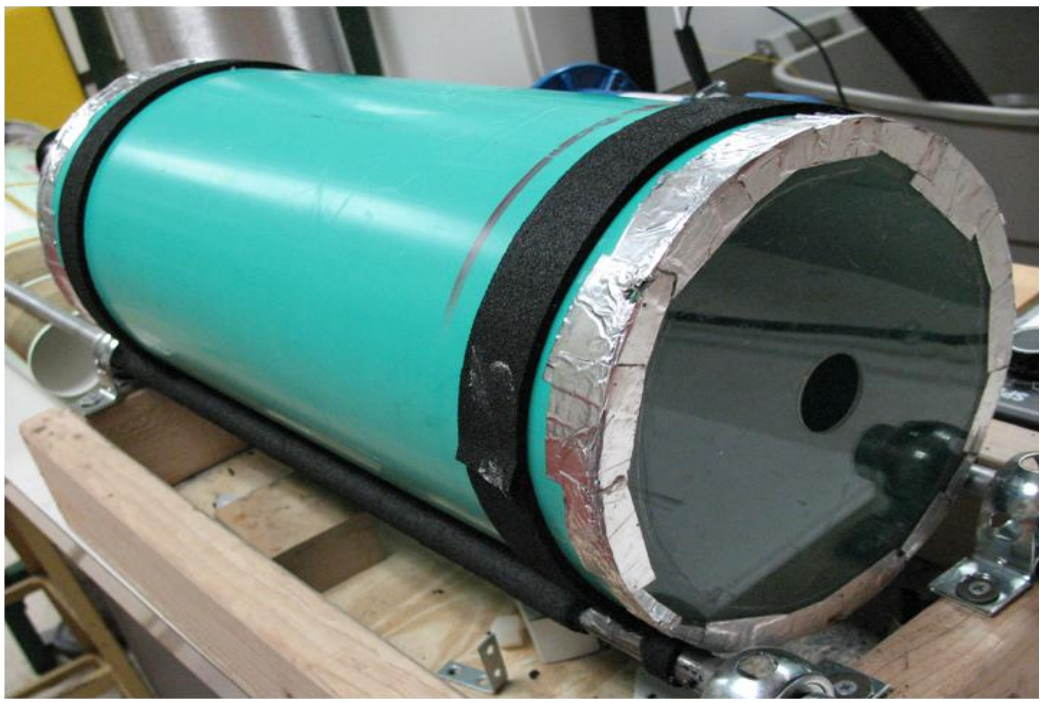

Figure 3.7: PVC cylinder with clear end caps positioned on the roller apparatus.

The model of the tank in Figure 3.7, can be rotated using the roller apparatus and a camera is directed at the clear end caps to record the flow field. In order to be visualized, the surrogate fluid has to be translucent with identical viscosity to the surfactant solution. The fluid consisted of carboxymethyl cellulose and water, with the concentration of carboxymethyl

cellulose adjusted to achieve the desired viscosity. To test the viscosity of both the surfactant and the substitute fluid, a column was built as shown in Figure 3.8.

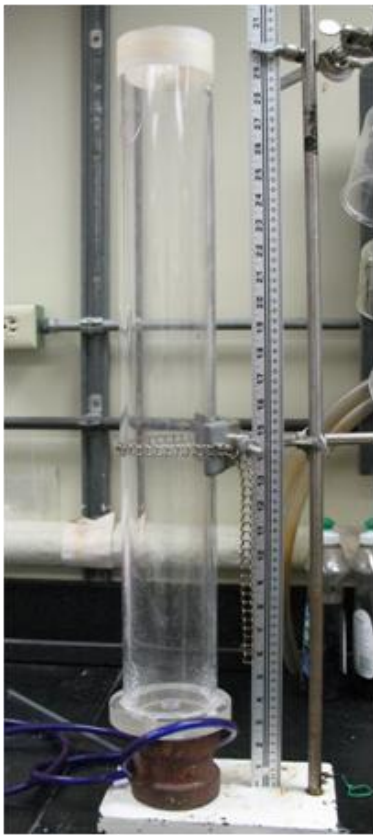

Figure 3.8: A column 64.77 cm tall used to measure the viscosity of a fluid.

The apparatus consists of a 64.77 cm tall column that is filled with liquid. The liquid height is measured and a glass sphere is placed at the top of the liquid. The sphere is allowed to fall and time measurements are taken to determine the velocity of the glass sphere. Assuming terminal acceleration has been attainted; measurements can then be converted into the viscosity of the fluid. To initial equations for determining the viscosity of the fluid is a force balance on the falling glass sphere, equation (3.7).

$$F_{buoyancy} + F_{drag} = F_{gravity} \qquad 3.7$$

The force balance is simplified with the use of the drag coefficient equation (3.8) which is used for moderate Reynolds number ($.01 < Re < 6x10^3$).

$$f = \frac{4}{3}\frac{gD}{v^2}\left(\frac{\Delta\rho}{\rho_{fluid}}\right) \qquad 3.8$$

where $\Delta\rho$ is the density difference between the sphere and liquid (1.535 g/cm^3), g is the acceleration of gravity (980 cm/s), D is the diameter of the sphere (4 cm), and v is the velocity of the sphere, ρ_{fluid} is the density of the surfactant solution (1.04 g/cm^3). The density of the glass sphere is 2.575 g/cm^3. The drag coefficient of a falling sphere calculated using equation (3.8) can be related to the Reynolds number of the falling sphere (equation 3.9).

$$f = \frac{18.5}{Re^{\frac{3}{5}}} \qquad 3.9$$

The relation is only valid at moderate Reynolds numbers and from the calculation it was determined that the Reynolds number for the falling sphere was 28.65. The Reynolds number is inversely related to the viscosity 3.10.

$$\mu = \frac{Dv\rho}{Re} \qquad 3.10$$

The surfactant solution has a viscosity of 525 cp, and 25.5% by mass carboxymethyl cellulose in water pseudoplastic (Bird, Stewart, and Lightfoot, 2002) that can be used as a surrogate aqueous solution for flow visualization.

The cylinder is filled with the surrogate fluid, and red plastic pellets (d≈1mm) are placed in the solution. The pellets have similar density to the fluid, 1.04 g/cm^3. The neutrally-buoyant pellets are entrained by the solution while the tank rotates, allowing for flow visualization to be completed using digital videography. The following figure illustrates the pellets inside the cylinder.

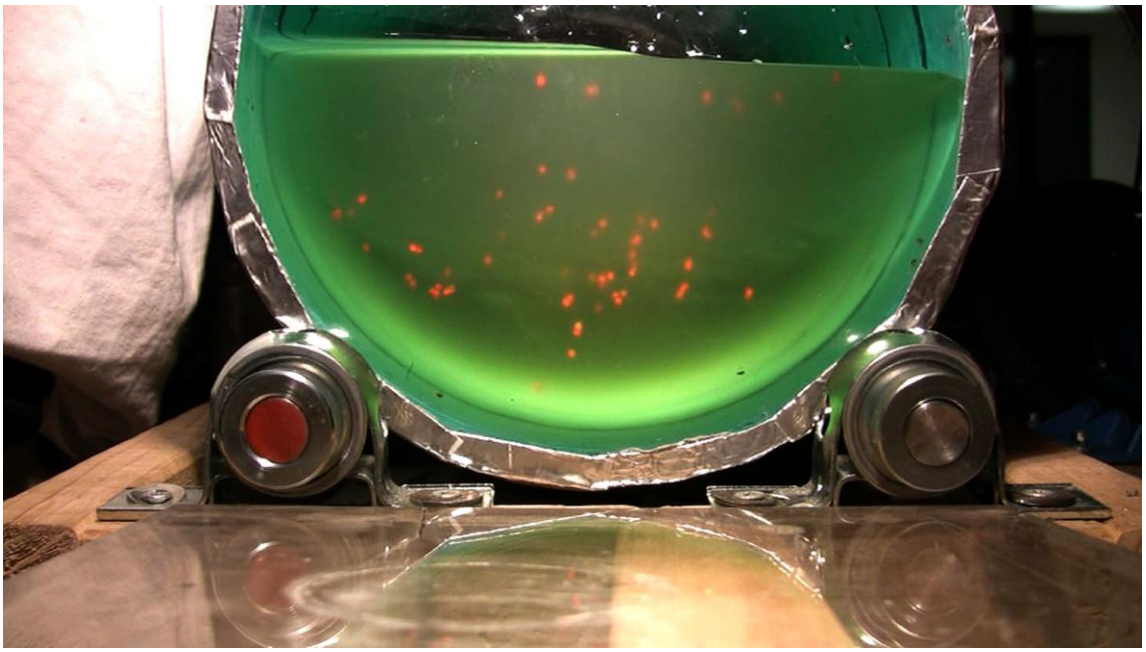

Figure 3.9: Pellets entrained in carboxymethyl cellulose liquid inside a half filled cylinder

The fluid-borne particles are easily seen in the tank and their position(s) can be monitored with time. The movement is measurable because the frame rate is 60 frames per second and

every fourth frame was used to record the flow pattern inside the cylinder. The outside edge of the cylinder was rotating at 6 rpm, so the tangential velocity of the cylindrical wall was 6.284 cm/s (0.20944 ft/s) .

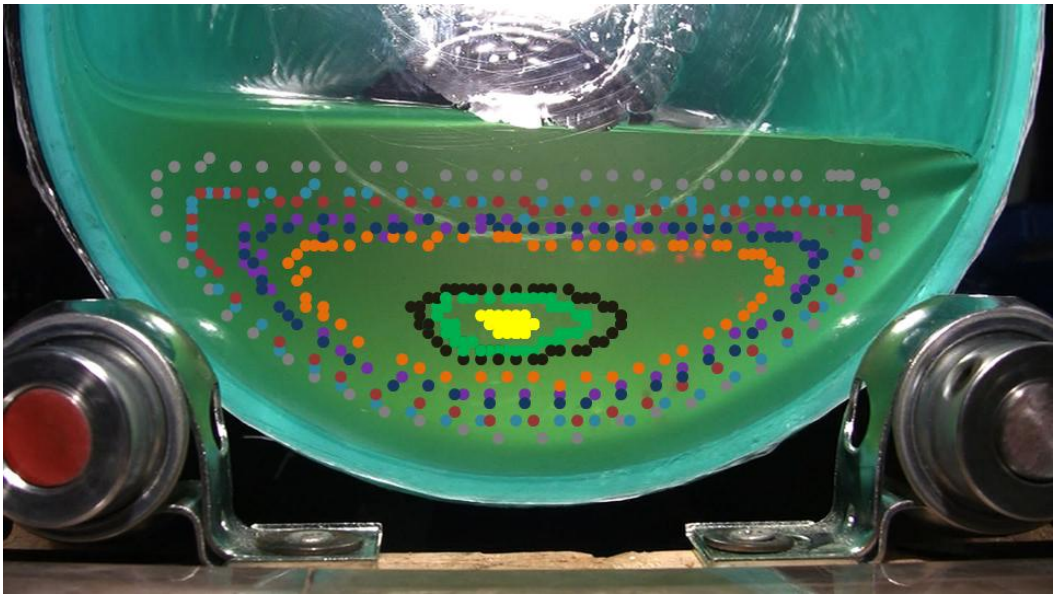

Figure 3.10: Flow visualization from the particles entrained in solution

An example of flow visualization is provided in Figure 3.10 and the velocity profile can be compared with equations 3.4 and 3.5. The following figures illustrate the θ and r- components velocity vector as computed from the model.

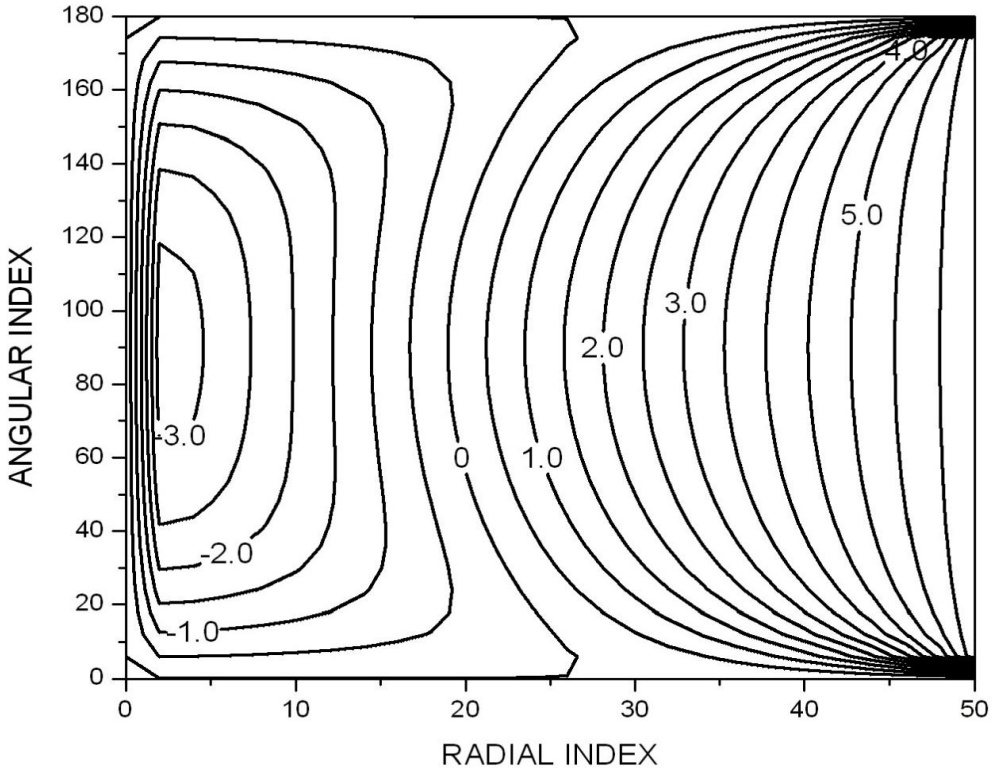

Figure 3.11: Computed θ-component of the velocity vector, with the labels corresponding to velocity (cm/s).

Figure 3.11 illustrates the cylindrical coordinate equation calculation for the angular component of the velocity profile (θ) and is plotted on a Cartesian plot. The top and bottom of the plot each represent half of the liquid-gas interface (free surface), and the right-hand side (radial index=50) corresponds to the wall-fluid interface.

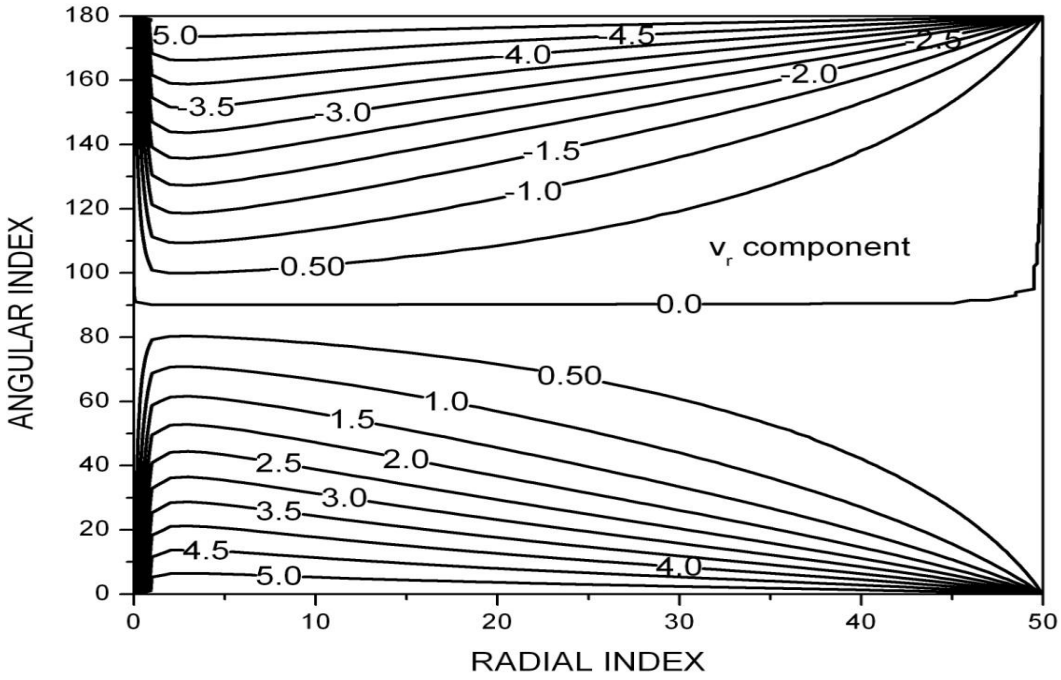

Figure 3.12: Computed r-component of the velocity vector. Again, the labels correspond to velocity contours (cm/s).

The r-component illustration, Figure 3.12, is also presented on a Cartesian plot and has identical spatial meaning as Figure 3.11. Figures 3.11 and 3.12 illustrate the velocity profile in the liquid phase, and the continuity equation is used to model the transport absorption of the solute.

After flow visualization, the modeling of the absorption of carbon dioxide into the surfactant solution was completed by solving Equations 3.4-3.6 simultaneously. Figures 3.13-3.15 below show how the carbon dioxide is distributed throughout the liquid phase for small positive time steps.

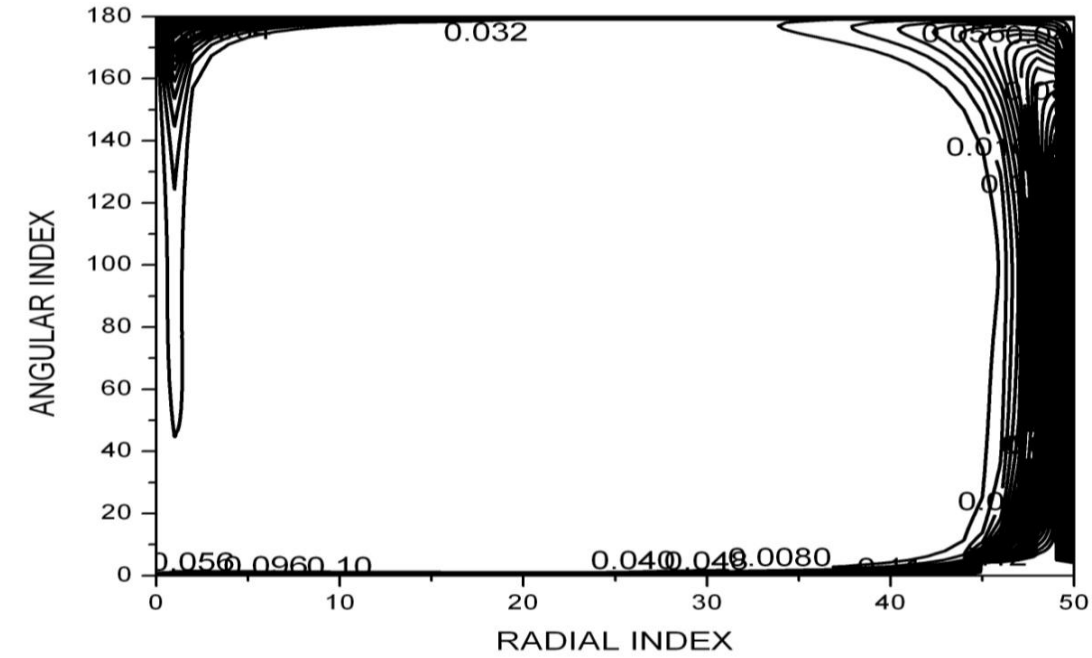

Figure 3.13: Concentration field in the liquid phase at t=5 sec.

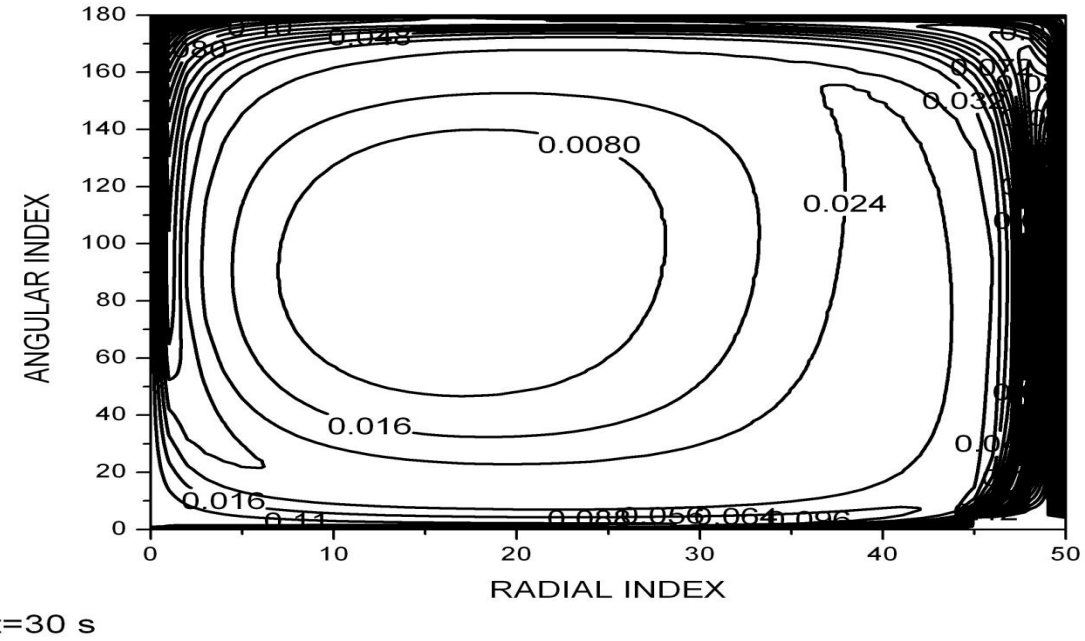

Figure 3.14: Concentration field in the liquid phase at t=30 secs.

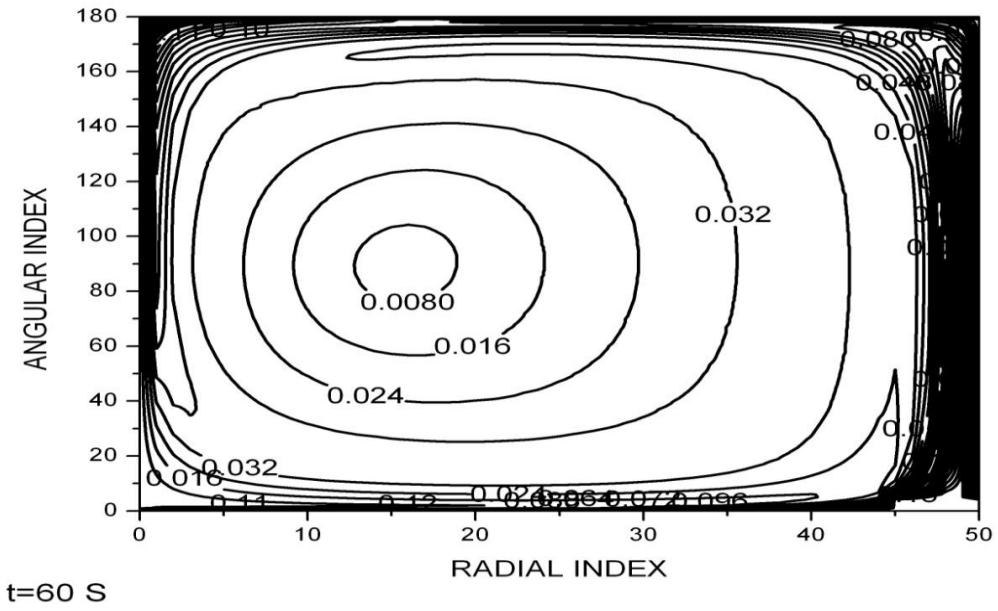

Figure 3.15: Concentration field in the liquid phase at t=60 secs

The modeling of the absorption process with respect to time shows that the transport of solute in the rotating cylinder is substantially faster than in the diffusion-limited case, as expected. This improvement in the rate of absorption resulted in a much more rapid approach to saturation and without the undesirable viscous heating.

Experimental Convective Absorption of Carbon Dioxide

The ability to improve the absorption process was critical to this work and to the feasibility of the entire system. To improve the absorption process a roller apparatus consisting of a motor, two rods, bearings, speed controller, pulleys, v-belt, and a wooden frame was built. The apparatus was developed to slowly rotate the cylinder at 6 rpm and Figure 3.13 is a picture of the roller apparatus.

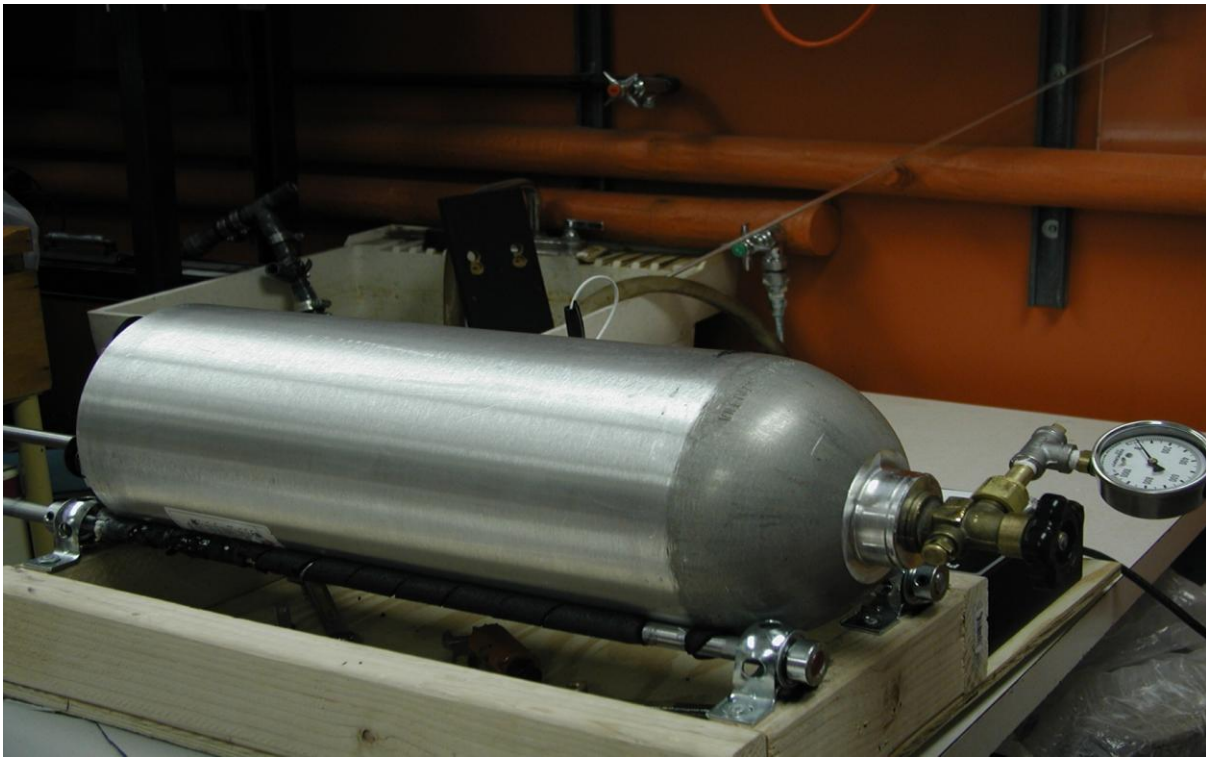

Figure 3.16: Rotating cylinder apparatus for improved absorption.

The cylinder rests on top of two roller bars which are positioned to prevent unwanted translation of the cylinder. The back rod is connected to a pulley on the left side and is attached to a variable-speed DC motor. A slight tilt is applied to the apparatus and a safety guard is position in the rear to prevent the cylinder from falling off the apparatus.

The experimental procedure consisted of preparing an aqueous surfactant solution and placing it into the aluminum (beverage) cylinder. The tank was pressurized with CO_2 to about 800 psi, and allowed to spin at about 6 rpm in a "horizontal" fashion. The amount of carbon dioxide absorbed could be monitored through the change in head-space pressure. With this arrangement, the mass transfer was both convective and diffusive. Furthermore, the interfacial area was the bulk fluid surface and the wetted surface in the head space. As the gas phase pressure decreased, the total amount of carbon dioxide that is absorbed into solution was determined. These calculations were identical to the diffusion-limited experiment, but the results were very different. The following figure displays the head space pressure of the rotated cylinder over eight repeated pressurizations.

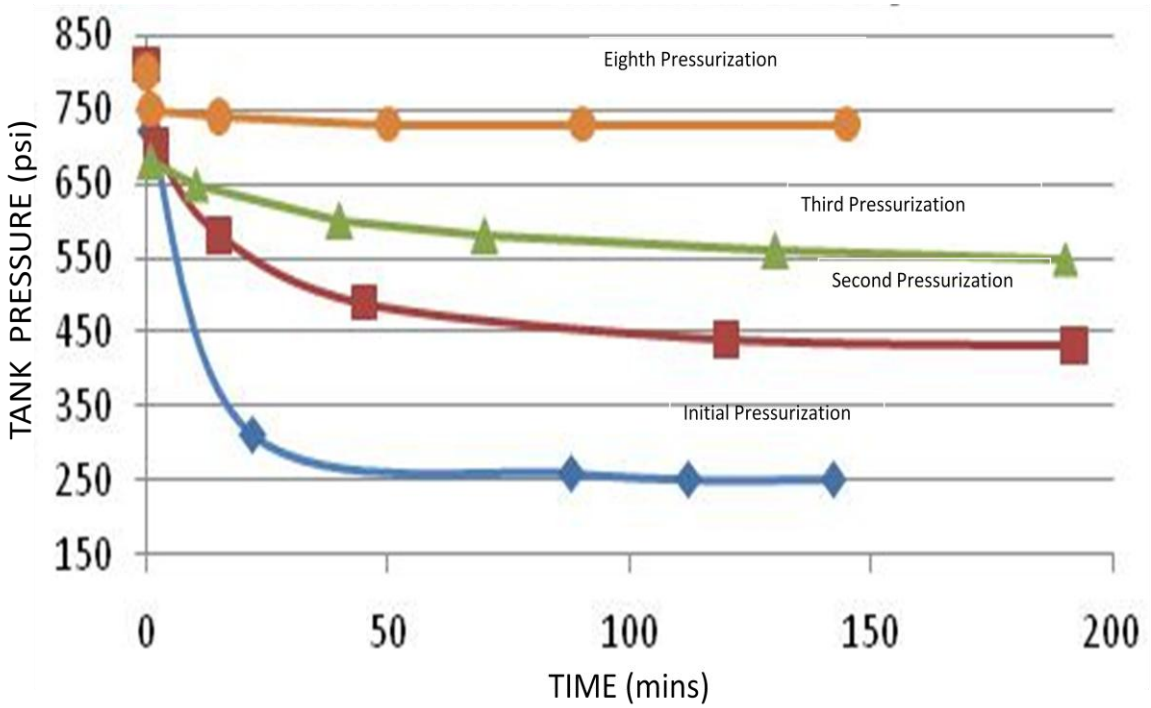

Figure 3.17: Tank pressurization history over eight repeated pressurization cycles with a total of 682.59 grams of carbon dioxide absorbed by the surfactant solution.

The rotation of the tank greatly reduced the experimental time that was required for the absorption of carbon dioxide into the surfactant solution. The figure shows that over eight pressurization cycles the surfactant solution approached saturation. The improved absorption process now required hours instead of days to achieve similar results.

The mass of carbon dioxide absorbed was greatly enhanced with the improved transport technique. To determine the mass of carbon dioxide that was absorbed, the ideal gas law is used on the change in head space pressure. This resulted in 682.59 grams of carbon dioxide being absorbed in 13.33 hrs, and also resulted in more foam being generated during the discharge process.

Conclusion

Two modes of absorption of carbon dioxide into the surfactant solution were studied: molecular diffusion and diffusion enhanced with fluid motion. Initially the diffusion-limited approach for mass transfer of carbon dioxide into the surfactant solution was considered. A model was developed and experiments conducted that determined the rate of absorption was too

slow to be feasible. The results from the experiment of diffusion-limited mass transport found that 116.59 grams of carbon dioxide was absorbed in 104 hours. These results were impractical for the intended application, so a new technique (horizontal rotation) for the absorption process was developed. It was determined that rotating the cylinder at 6 rpm would result in 682.59 grams of carbon dioxide being absorbed in 13.33 hrs (if T≈77ºF). This was a 6-fold increase in the carbon dioxide absorbed in one tenth of the time. This improved absorption resulted in both an increased amount of carbon dioxide absorbed and better foam volume.

CHAPTER 4 - Air Induction System and Foam Ingestion

The goal of this project is the development of a stand-off system of minimum lethality, but one capable of stopping an approaching automobile or light truck and rendering it inoperable for at least 10 minutes. To accomplish this task a foam spray is being developed that would enter the air intake system of automobile, disrupt combustion, and occlude the pores of an air filter. Before experiments can be contemplated, information on automobile air intake system is needed.

Standard automobiles require 0.0283-0.0566 m^3/s (1-2 ft^3/s) of air flow to support combustion in an engine. The air is drawn in through an air induction port (in a variety of positions, but typically under the hood). The air then travels through ducting to the air filter. The filter prevents particles and other foreign objects from entering the combustion chambers, thus preventing damage to the pistons and other engine components of the automobile. A picture of an induction system (a Jeep Liberty in this case) can be seen in Figure 4.1.

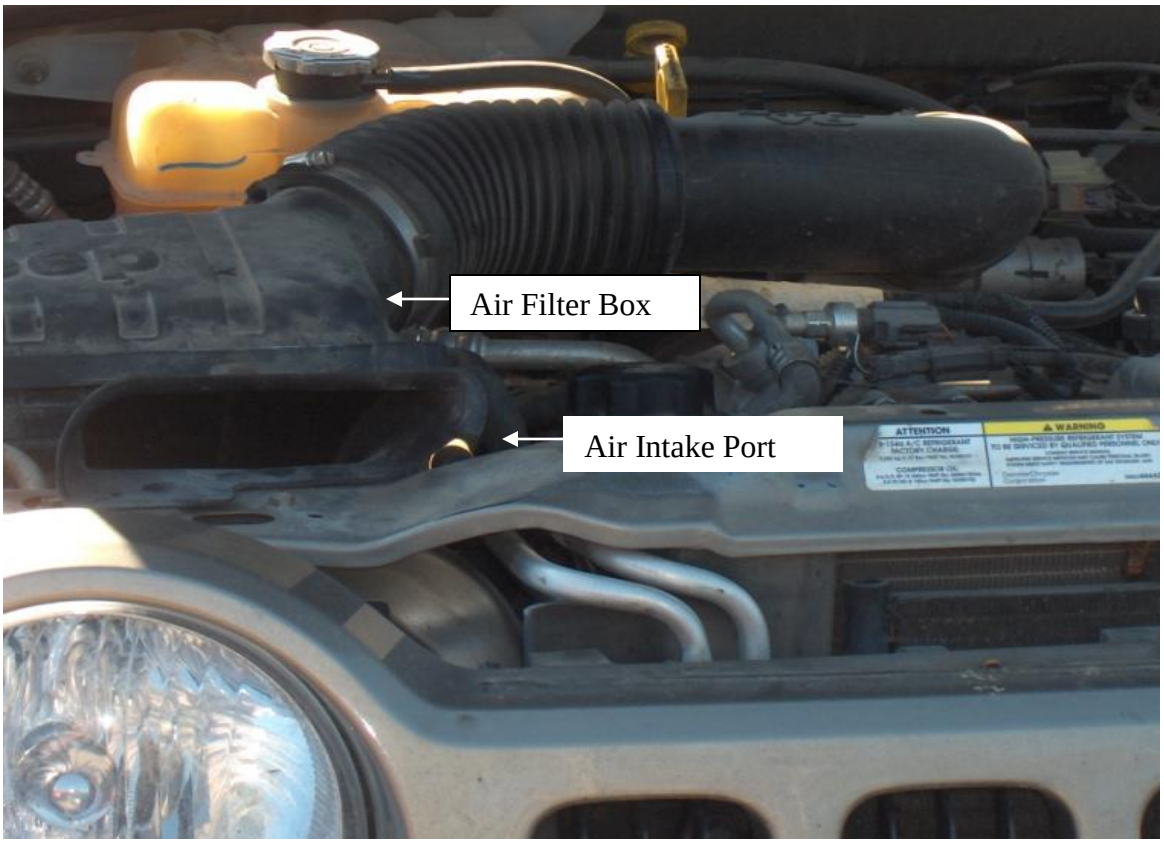

Figure 4.1: A picture of an air induction system of a Jeep Liberty

Figure 4.1 clearly shows both the location of the air intake port and the filter box for a Jeep Liberty. The dimensions of this intake port are approximately 17.8 cm by 5.1 cm. The air flow rates for typical induction systems for a range of engine sizes are provided in table 4.1.

Table 4.1: Air intake characteristics based on size of the engine (idling at 1000 rpm)

Liters Displacement	CID	Aspirated Volume, Cubic m/min	Intake CFM	Average Intake Velocity, m/s
2	122	1549.4	35.3	4.30
3	183	2324.1	52.9	6.45
4	244	3098.8	70.6	8.61
5	305	3873.5	88.3	10.76
6	366	4648.2	105.9	12.91
7	427	5422.9	123.5	15.06

The table shows that typical air intake velocities are between 4.30 to 15.05 m/s. This velocity range has the potential for foam deformation and translation. Experiments were conducted to determine the ease with which foam will be drawn into the induction system, and the results are presented in the following sections.

Decreasing the oxygen concentration and blocking the air flow through the induction system can be accomplished with a foam spray that engulfs the air intake of an automobile and occludes the pores of the air filter media. To test the ability of the foam to perform its given task, experiments had to be conducted on the shear stress developed at an automobile air intake, the ability of foam to deform and translate, and the discharge of foam from a pressurized cylinder. The air intake system also needed to be replicated to check the full-scale feasibility of the non-lethal system.

Velocity Profile and Shear Stress of an Air Intake System

The vehicle stopping system requires foam to travel through ducting and into the air filter box after entering the intake system at the air intake port. The air flow through the air intake port will exert a shear stress on the foam. To determine the amount of shear stress that occurs while

the foam is being ingested into the air intake system, a facsimile air intake was constructed. Figure 4.2 is a picture of the facsimile air induction system.

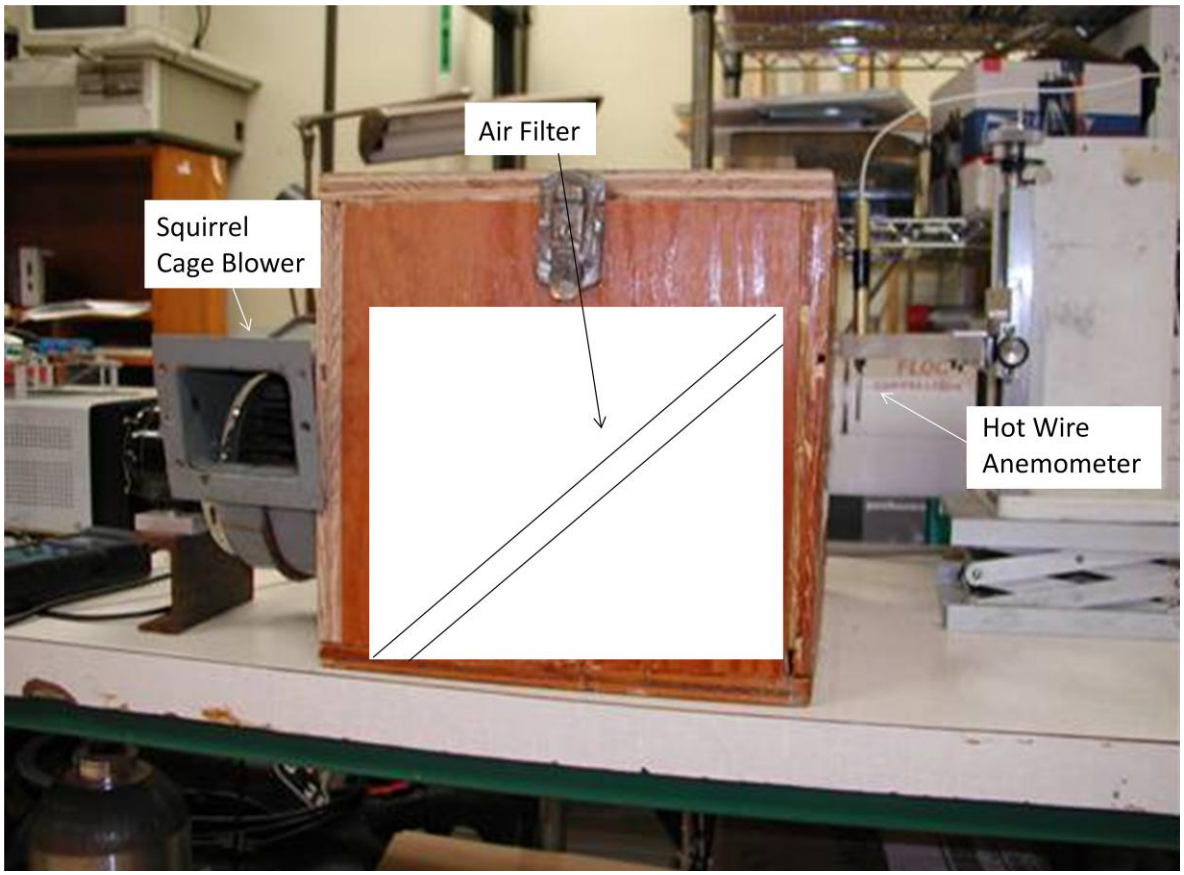

The facsimile air intake system was built using a wooden box equipped with a squirrel-cage blower controlled by a Variac. The blower induced flow of air through the air induction port that was cut into the wooden box on the left side. The velocity is measured using a hot wire anemometer and the output of the sensor can be converted into air velocity.

Figure 4.3: The air induction port and hot wire anemometer in position.

Figure 4.3 is a picture of the air intake port and hot wire anemometer that is attached to a x-y (2D) positioning apparatus. The air induction port was modeled after the air induction port of a standard vehicle. The opening was 5.08 cm x 15.2 cm and the velocity could be measured for both vertical and horizontal traverses. This configuration of the blower, as well as the air intake port, led to eddies being formed throughout the air box. These eddies adversely affected the velocity distribution at the air intake, producing inconsistent data from the hot wire anemometer. To solve this problem, an air filter was added to the box, causing the turbulence in the flow regime to be reduced and resulting in flow that is similar to an automotive air induction system. Figure 4.4 is a picture of the facsimile air filter box with an air filter added. The filter alters the air flow to create a more symmetric velocity profile at the air intake port.

The air velocity of the intake system was adjusted, and measurements were taken of the average point velocity along the intake port. A Variac was used to regulate the voltage to the air blower and allowed the velocity to be varied from 1.5 to 8 m/s at the center of the air induction port. The anemometer was moved from 2.54 cm below to 2.53 cm above the intake in 0.508 cm increments to record the velocity profile. The main focus during the

Figure 4.4: Addition of an air filter improved the velocity distribution.

experiment was the horizontal centerline velocity distribution because it would give the highest shear stress for the foam. Figure 4.5 is the distribution of time averaged point velocities at the horizontal centerline of the air intake.

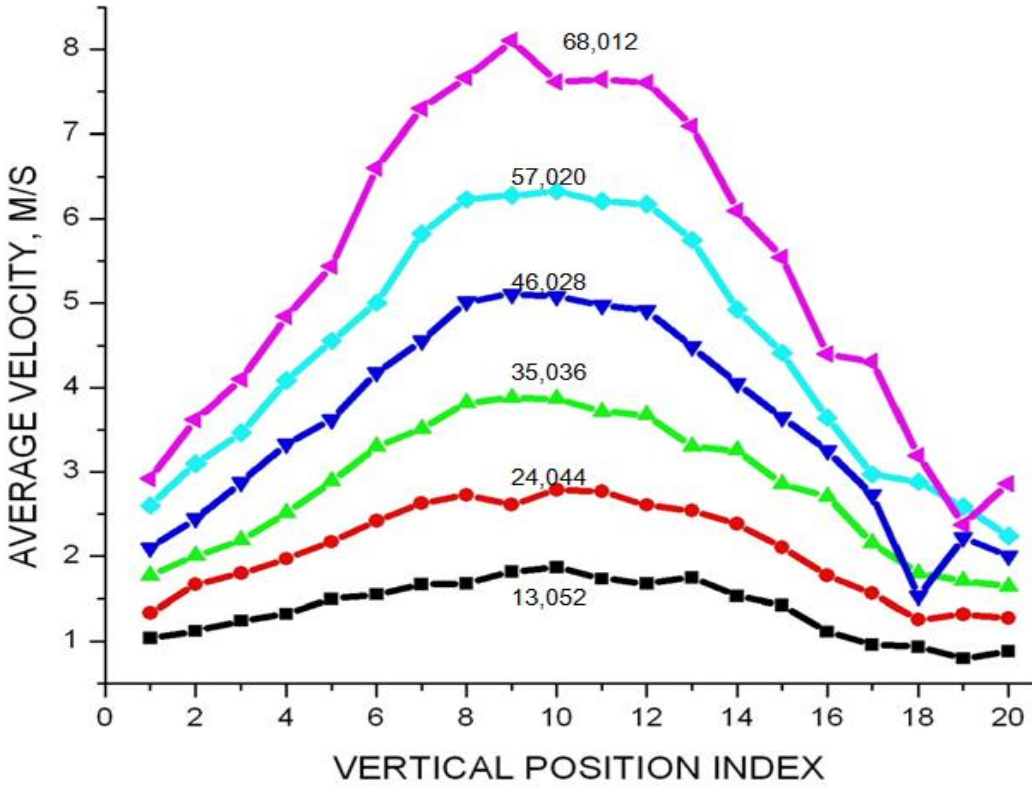

Figure 4.5: Velocity distribution for the air induction system at the horizontal center (7.62 cm) with volumetric flow rates ranging from 13,052 to 68,012 cm^3/s.

Calculations on the shear stress were completed and figure 4.6 is the illustration of the results. The shear stress calculations are based on the change in velocity with respect to position, $\tau_{yz} = -\mu \frac{dV_z}{dy}$.

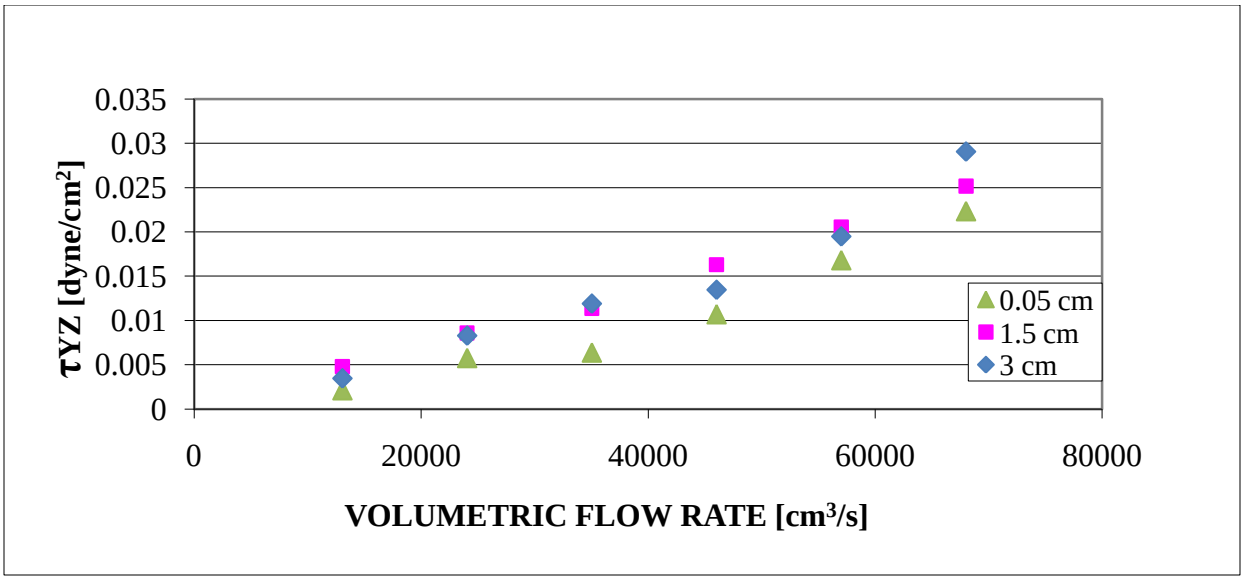

Figure 4.6: Shear stress calculation at horizontal positions .05, 1.5, and 3 cm

The maximum shear stress (0.03 dyne/cm^2) at the horizontal centerline (x=3 cm) occurred at y=0 (the edge of the port) and the highest velocity (7000 cm^3/s).

Flow Experimentation

The air induction system of an automobile has a duct that the foam must flow through before it enters the air filter box. To test the foam's ability to block the air induction system of an automobile, the stability and flow of the foam must be characterized. To perform this experiment, a foam collection system was designed to hold the foam until a vacuum was applied. The foam would then be drawn through a 1.93 m (6 ft) tube with an air filter at the end of the system. This would test both the foam's ability to occlude the pores of an air filter media and to flow through the air induction system. These two foam characteristics are crucial for understanding of the mechanisms and implementation of the non-lethal system.

The testing was conducted using a camera for flow visualization and pressure sensors that measured the vacuum pressure along the tube. The data from pressure sensor were analyzed to determine the instant the foam blocked the air intake system. The following figure is a picture of the foam collection system and tubing for the air flow experimentation.

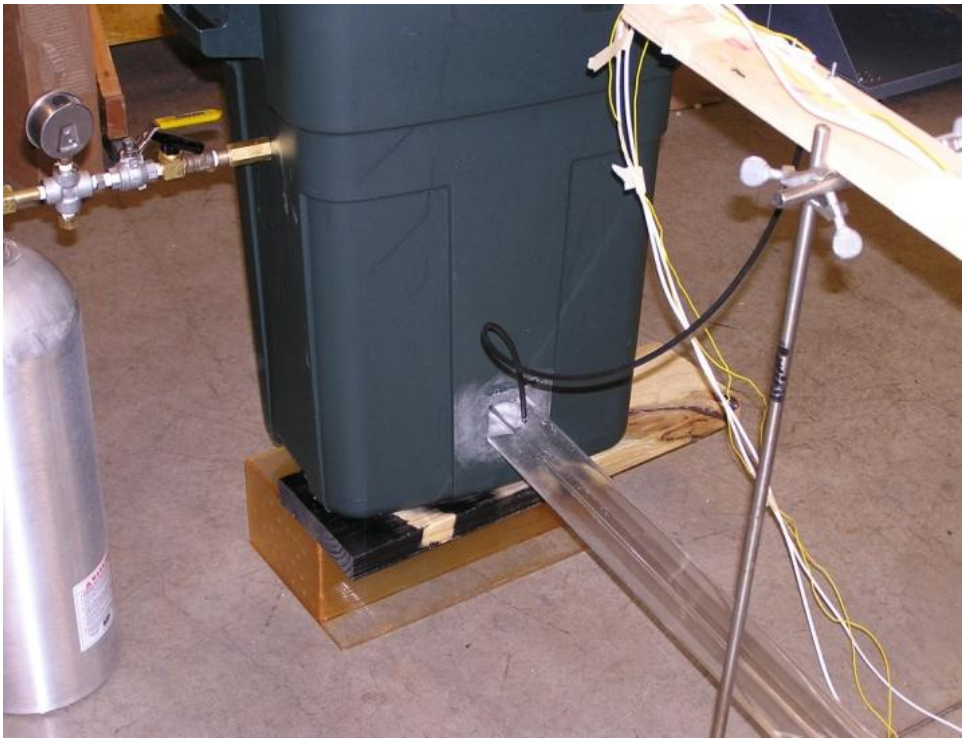

Figure 4.7: Apparatus for evaluating foam deformation and flow in a square (4.35 by 4.35 cm) acrylic plastic duct

The figure is a picture of half of the apparatus and it shows the tank next to the foam collector. The device collects the foam from the cylinder and measures the volume of foam produced. Once the foam has been collected, it can then be drawn into the mock air induction system using a shop vacuum. The pressure is monitored using four pressure transducers that are located next to the collector, the midpoint of the six foot duct, next to the air filter box, and beneath the air filter. The output of the pressure transducers are monitored with a data logger to determine if and when the foam has clogged the filter.

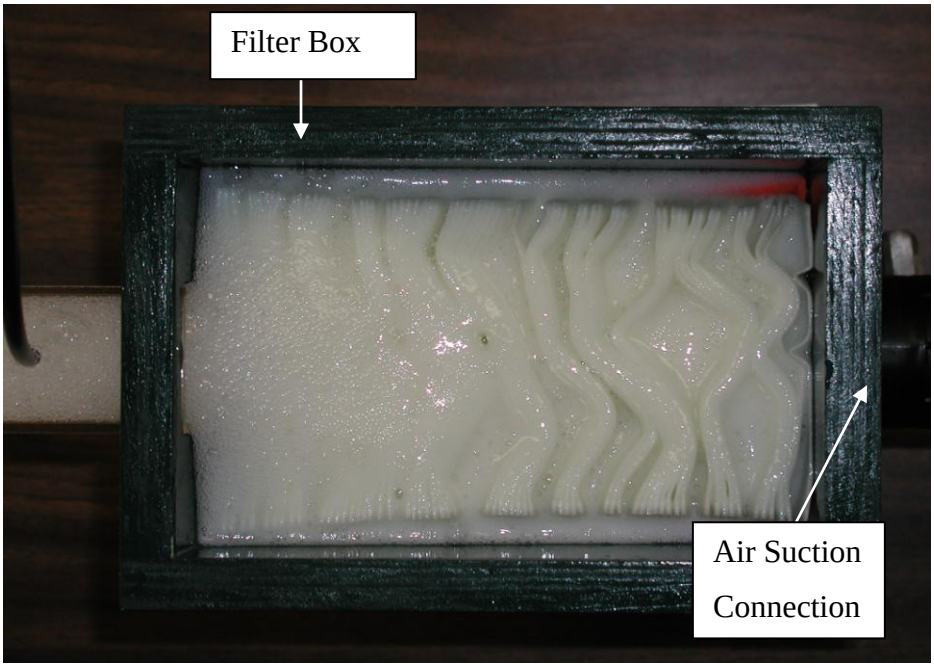

Figure 4.8: Air filter box with suction connection

Figure 4.8 shows the air filter box, the suction connection, and the 6 foot pipe connection used in the flow experiment. This air filter box provides the setup to characterize the flow of the foam and the confirmation that the foam occludes the pores of the air filter medium. Figure 4.9 illustrates the static foam orientation under the effect of gravity and a very small head pressure. Once the suction is turned on, the fluid is forced down the length of the pipe by a vacuum. The foam then enters the air filter box, shown in Figure 4.8, and rapidly disrupts air through the filter. Pressure sensors are used to determine the time it takes the foam to both flow to the air intake and occlude the filter. As soon as the vacuum is turned on, the pressure gauges respond and the pressure will decrease. When the

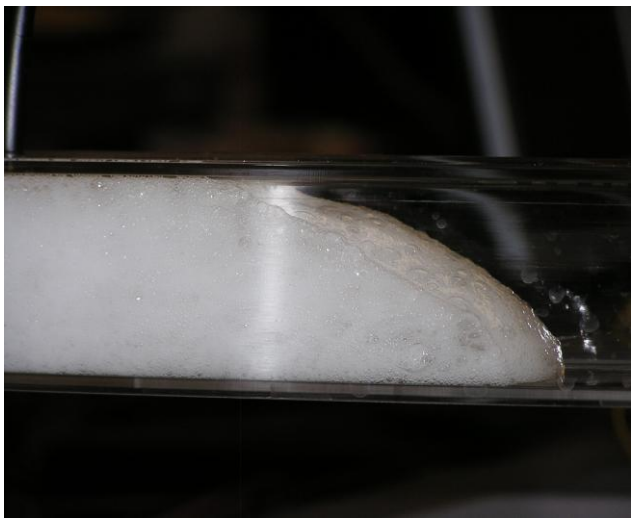

Figure 4.9: Static foam orientation in square duct prior to suction.

air filter becomes blocked, the pressure sensor under the filter maintains vacuum, while the other three sensors lose vacuum pressure. Figure 4.10 illustrates the experimental results from one of the trials.

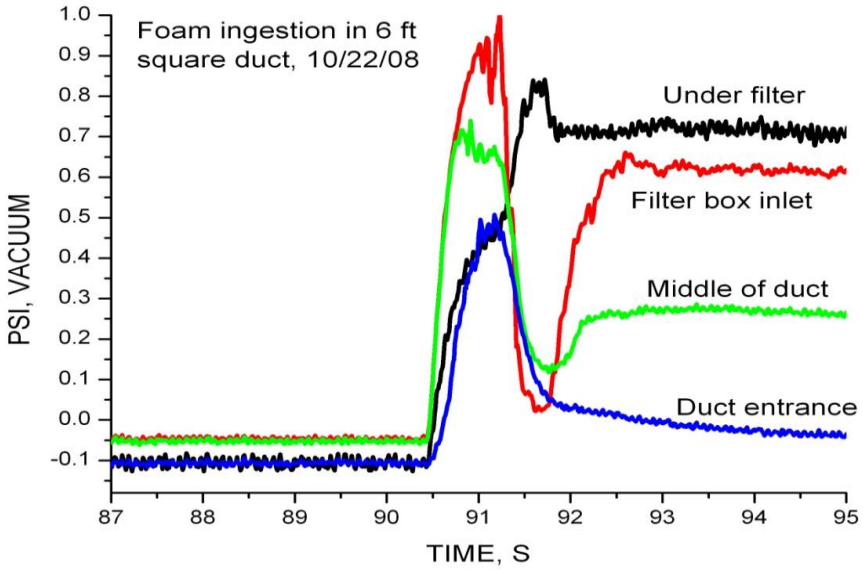

Figure 4.10: Dynamic record of pressure in the test section and underneath the air filter. Flow through the system was initiated at t=90.4 s, and filter (pore) occlusion was complete by t=92 s.

Figure 4.10 shows that the experiment blocked the air filter in less than 2 seconds. It can be seen in the figure that the vacuum started at t=90.5 seconds. The foam then traveled the length of the tube, which resulted in the filter being occluded within one second of the initial vacuum being applied. The figure also demonstrates that the pressure under the filter increased after it was blocked. The reason the vacuum pressure was not maintained after the pores of the filter were occluded was because of filter deformation from the force of the vacuum. Figure 4.11 shows the filter after contact with the foam.

Figure 4.11: Top and side view of an air filter after contact with foam. The bottom image shows the deformation of a full-sized Fram™ air filter resulting from foam ingestion.

Once the foam has contacted the air filter, the foam solution occludes the pores of the filter, and if the vacuum is maintained, the filter becomes deformed (the supporting steel mesh is bent). The top part of Figure 4.11 shows how the filter pleats stick together. The deformation of the filter can be seen in the bottom half of the figure. Figure 4.10 and 4.11 demonstrate the consequences of the foam entering the air induction system and the response of the filter media. This degree of blocking the air filter is more than sufficient to choke the intake of a car.

The results from these experiments demonstrate the predicted response of an automotive induction system to foam ingestion. These experiments demonstrated the foam's behavior in a real-world application and the flow rate of the foam through the air induction system. This also

demonstrates the suitability of the foam's composition to immobilize the vehicle by restricting the air intake flow, the main objective of this project.

Tank Discharge Characteristics and Experiments

A prepared surfactant solution was pressurized with carbon dioxide and then released to the atmosphere. The dissolution of carbon dioxide during the discharge results in foam being formed. The dissolution process is affected by the foaming nozzle and the control valve (mass flow rate). The control valve was adjusted in several experiments were conducted to determine the discharge rate effects on the production of foam. These experiments consisted of velocity distribution of the discharge, discharge valve characteristics, and the pressure drop across the valve.

Velocity Distribution of Discharge

When the foam is released from the highly pressurized beverage cylinder, the foam is discharged at a high velocity. The foam will then form a cone-shaped discharge because of the foaming nozzle that has been attached to the device. The velocity distribution of the foam release was measured and the foam discharge characterized. A high definition digital video camera, a pressurized beverage cylinder with the surfactant solution, and a ruled background were used to study the discharge characteristics.

The experiment was conducted by filling a cylinder with surfactant solution and then pressurizing the cylinder with carbon dioxide as discussed in Chapter 3. The tank was then discharged at a specific valve position and the discharge time was recorded. The shutter speed was adjusted to ensure the speed of the foam could be determined by streak length. Figure 4.12 is a picture of the initial discharge and Figure 4.13 is $1/60^{th}$ of a second later.

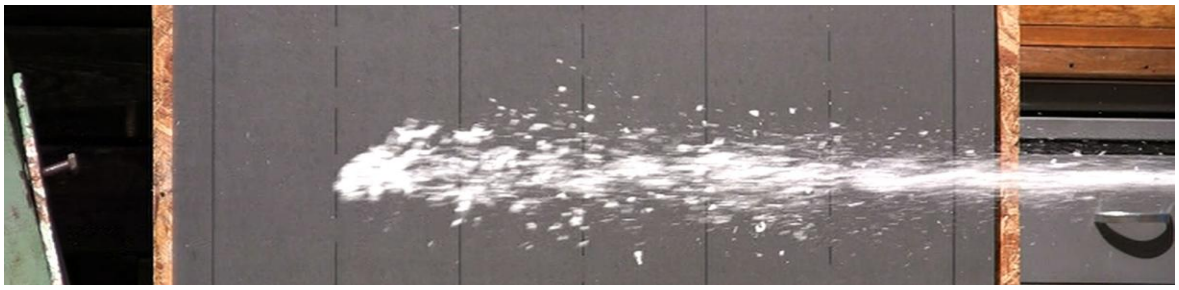

Figure 4.13: Still from video record of foam discharge at high rate.

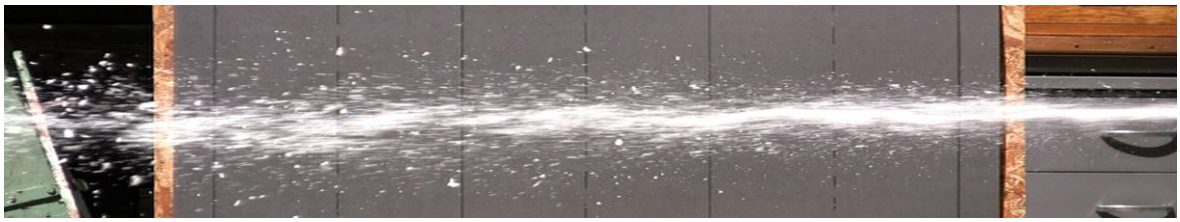

Figure 4.12: 1/60th of a second after first still from the video record of foam discharge at high rate.

The background board was marked every six inches, with a total length of three feet. The valve position controls the discharge rate. Trials at different discharge rate were conducted to optimize the foam volume from the cylinder. The following figure, Figure 4.14, illustrates a slower discharge rate of foam then the previous two images.

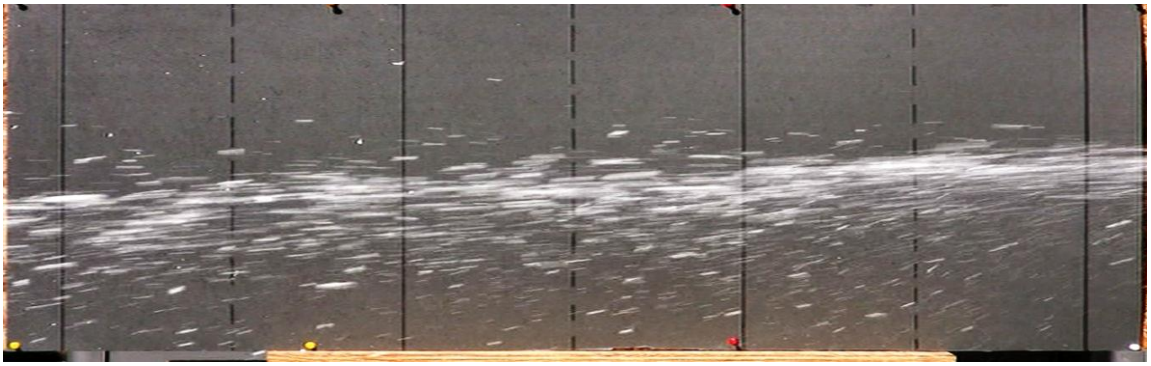

Figure 4.14: Still video image of foam discharge from pressurized cylinder with a centerline velocity of 15.31 m/s.

The comparison resulted in both the rate of discharge and the dispersion of the foam to be identified. The primary measured variable of this experiment was the velocity of discharge, which is compiled in Figure 4.15.

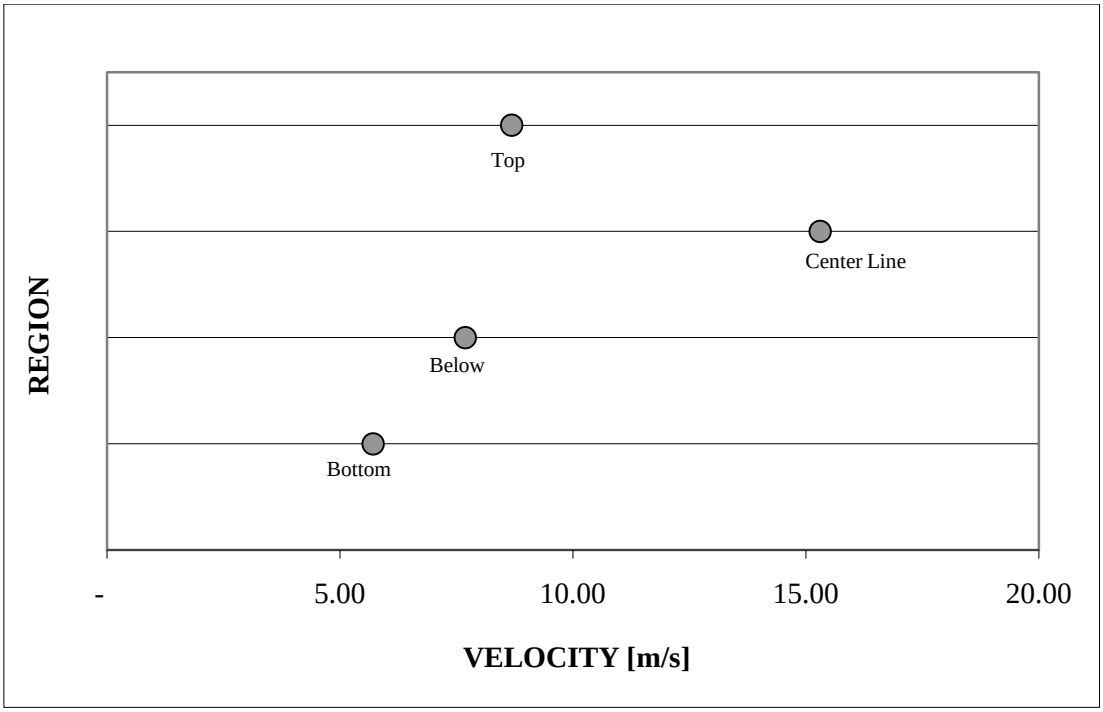

Figure 4.15: Average velocity distribution of four sectors of foam discharge for identical flow rate as Figure 4.14.

The qualitative velocity distribution shown in Figure 4.15 indicates that the velocity at the centerline of the foam discharge was about 15.31 m/s. This velocity distribution was for valve position 28, not a full open throttle valve for the foam discharge. The centerline velocity illustrated in Figures 4.12 and 4.13 was about 25.9-27.43 m/sec. This high rate of discharge was ineffective because the foam did not develop. Therefore, a decreased flow rate was used to generate foam, because it allowed the foam to fully develop and creates the largest foam volume. The discharge distance could be calculated from the velocity profile and it was estimated to be 6.1 to 9.14 meters from the desired target. This velocity distribution was critical because the optimum discharge rate could be identified, and the feasibility of the system verified.

Valve Characteristics

The discharge of foam begins with the surfactant solution traveling through the dip tube from the bottom of the beverage cylinder. The dip tube is connected to a piping network that includes a cylinder valve, a pressure gauge, a pressure relief device, two valves, and a foaming

nozzle. The cylinder valve is fully open and exerts no control over the discharge rate. The pressure gauge monitors the pressure of the cylinder. The discharge process is controlled by the two control valves and the foaming nozzle. The control valves determine the rate that foam will be discharged. The two control valves are in series, with one valve as a safety check and the second controlling the rate of discharge. The second valve is the primary valve that needs to be characterized to determine the optimum release characteristics.

The characteristic of the throttling valve impacts the rate of the foam discharge and the expansion of the foam. If there is no resistance to flow, the foam exits at a high flow rate, but the foam volume is reduced. The operating characteristics of the valve were assessed by calculation of the friction loss factor. To calculate the friction factor an approximation of the steady-state macroscopic mechanical energy balance is used, Equation 4.1.

$$\frac{1}{2}(v_2^2 - v_1^2) + g(z_2 - z_1) + \int_{p_1}^{p_2} \frac{1}{\rho} dp = \widehat{W}_m - \sum_i \left(\frac{1}{2} v^2 \frac{L}{R_h} f\right) - \sum_i \left(\frac{1}{2} v^2 e_v\right) \qquad (4.1)$$

The equation is simplified by assuming the velocity is constant ($v_2^2 - v_1^2 = 0$), the height is constant ($z_2 - z_1 = 0$), no work done by the surroundings on the valve ($\widehat{W}_m = 0$), and it was assumed that the friction loss of the tubing is minimal ($f = 0$). The approximation for the friction loss of the valve was given by Equation 4.2.

$$\frac{2P}{\rho v^2} = e_v \qquad (4.2)$$

The results of the friction loss experiment and calculations are presented in Figure 4.16

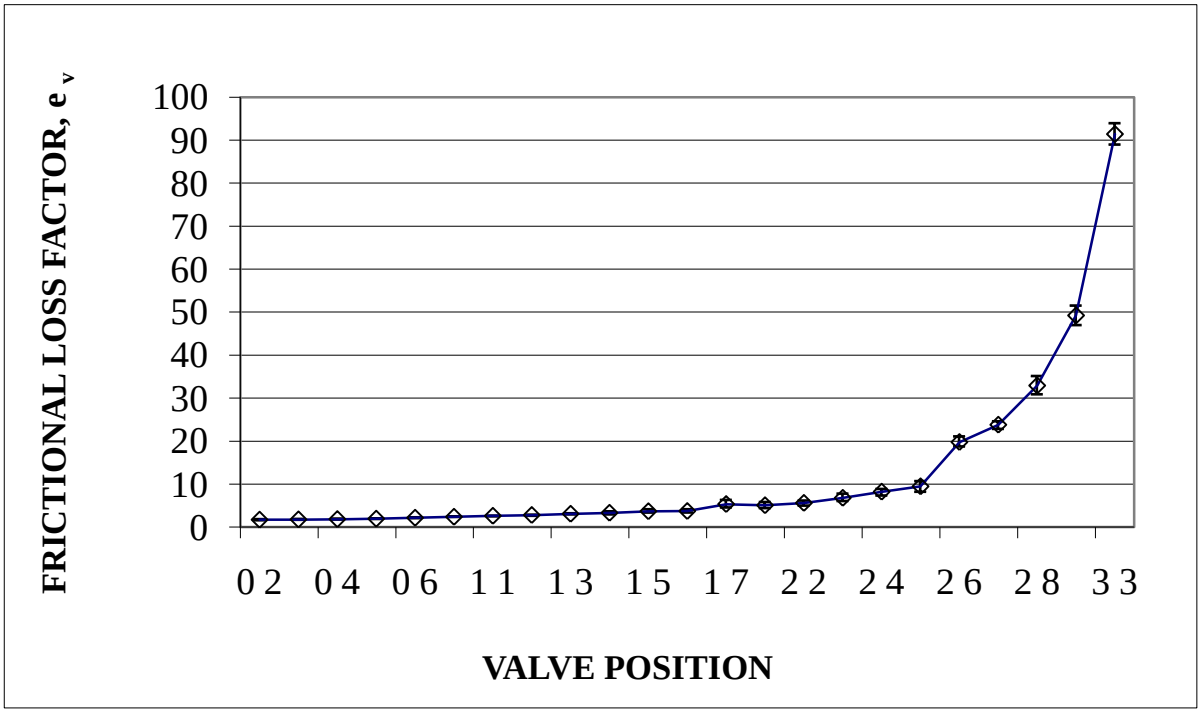

Figure 4.16: Experimental study of resistance offered by the principal discharge valve. Note that the loss is concentrated in a very narrow band of valve (stem) positions.

The above figure, Figure 4.16, shows the friction loss factor of the valve; position 0 corresponds to a fully open and position 33 to fully-closed. Each valve position represents an angle of 1.37 degrees. The fiction loss factor is the drop in pressure associated with friction of fluid flow. The figure shows that the valve had very little control and only when the valve approached the closed position did the friction loss factor increase substantially. Setting the valve accurately was very difficult; therefore in future experiments the valve position was set based upon pressure drop.

Pressure Drop across the Throttling Valve

The pressure drop across the throttling valve is an important factor in determining the amount of foam that can be produced. The valves enhance the interaction of the chemical species and increase the dissolution of carbon dioxide from the surfactant solution. To measure the dynamics of the valve, pressure transducers were added to each side of the control valve, which measured and recorded the pressure drop across the valve. The discharged foam is collected and the volume is monitored with time. This visualization of the foam volume can be correlated with the pressure to determine the best discharge rate. The experimental procedure consists of setting the valve position by looking at the pressure drop across the valve. After the valve is set, the

foam is released and a visual record is taken as well as data taken from each pressure transducer. The transducer output is then converted to pressure, and the pressure across the valve can be calculated. The pressure drop across the valve is shown in Figure 4.17.

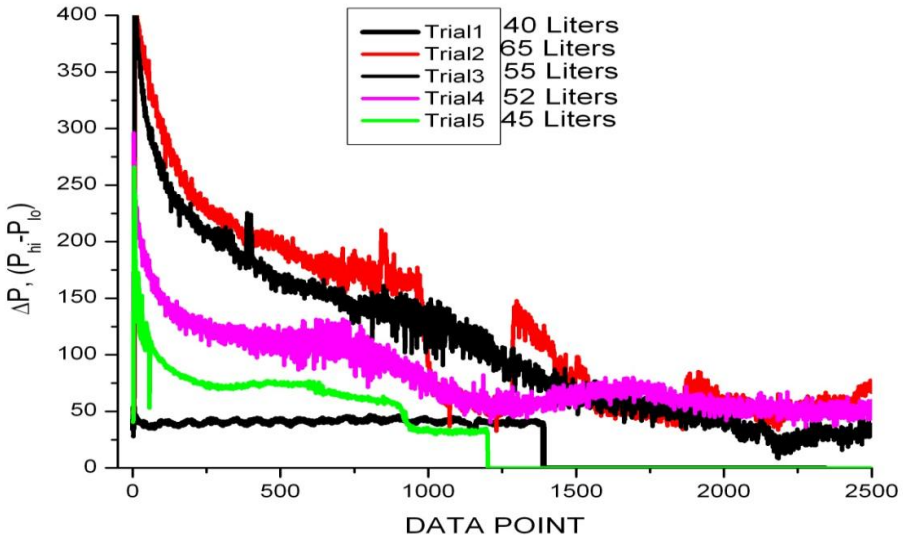

Figure 4.17: Effect of the discharge history (pressure profile) upon volume of foam produced.

Each trial In Figure 4.17 corresponds to a different valve position and is directly related to the discharge rate. A summary of the results can be seen in Table 4.2.

Table 4.2: Foam volume vs valve position

Trial Number	Valve Position	Total Foam Volume (L)
1	0	40
2	28	65
3	26	55
4	24	52
5	22	45

Table 4.2 shows the relationship between the valve position and the volume of the foam that was produced during the discharge. From Figure 4.17, the pressure drop that corresponded to largest volume of foam produced was valve position 28. If the valve is further closed to positions 30-33, the foam's volume from the cylinder is greatly decreased.

Figures 4.16 and 4.17 highlight the valve characteristics that can increase the quantity of foam. These experiments determined the optimum valve position for the production of foam. The results proved that a viable foam product can be produced from the prototype system.

Half Scale Automobile Intake Model

The final experiment that was conducted to assess foam ingestion was a half-scale model for an automobile intake system. The half-scale model has similar air intake port and air filter box dimensions of a Jeep Liberty. The model corresponds closely with an automobile intake system because of the desire to test foam ingestion and to validate the objective of the project (vehicle stopping

Figure 4.18 is a picture of the apparatus that represents a half scale model of an automobile engine. The air intake system has the same air intake port and filter box dimensions, but the air intake compartment is limited to half scale of an automobile compartment. The air is drawn through an air box by a vacuum generated by a portable shop vacuum. Additional equipment was used to do further testing, including pressure sensors and a camera. Pressure transducers were added to the air intake system to record the pressure as the foam traveled through the intake system. There are a total of four pressure transducers that are connected to the air intake. The pressure sensors are located at the inlet, in the middle of the piping, end of the inlet, and after the filter. Each pressure transducer records the pressure at a point along the intake.

Figure 4.18: Half scale model of the induction system apparatus without pressure sensors.

Figure 4.19 shows a close-up of the intake system with four pressure transducer connections added along the intake system. The pressure transducers, along with video evidence of the intake process, allow an understanding of the ingestion of foam. The pressure transducer determines when the foam is no longer being drawn into the air intake system. The pressure recordings can be seen in Figure 4.20.

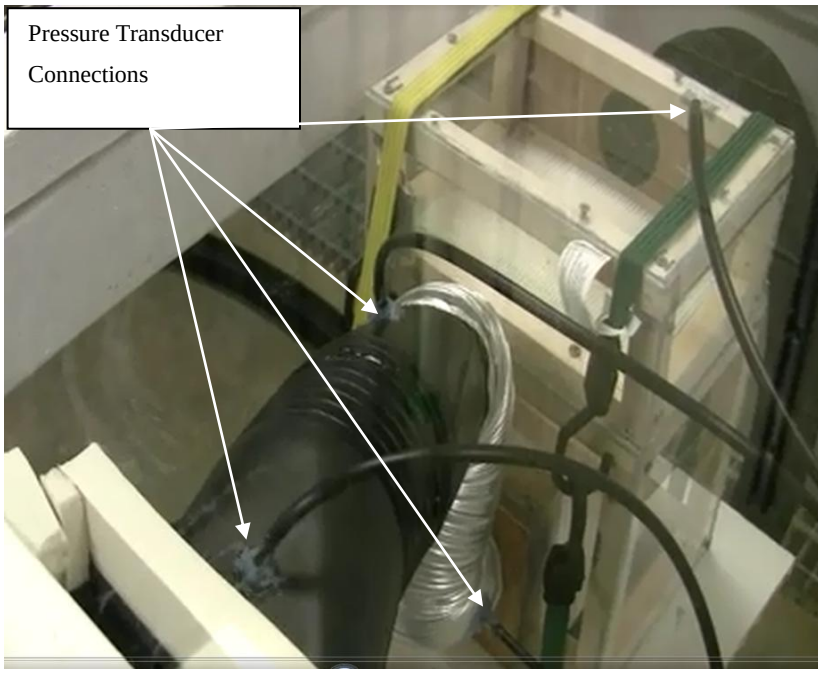

Figure 4.19: Half scale model of the induction system with pressure sensor ports.

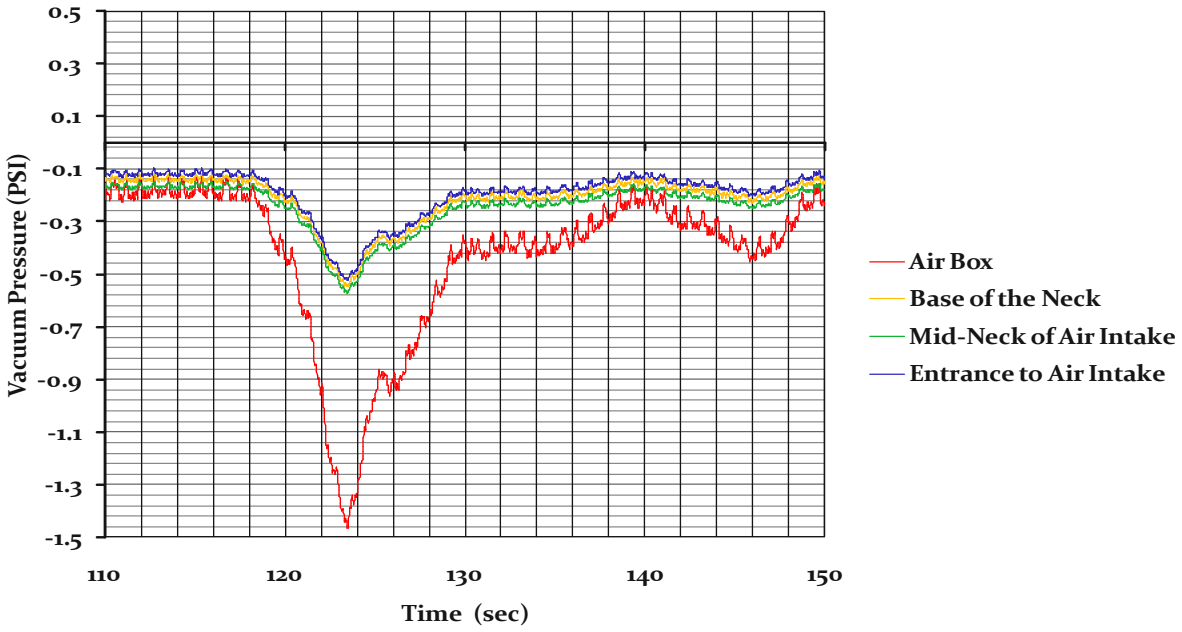

Figure 4.20: Dynamic record of pressure in an induction system model. Flow through the system was initiated at t=118 s, and filter (pore) occlusion was complete by t=124 s.

The pressure data show at t=118 seconds the foam was applied to the apparatus and after six seconds the foam had completely blocked the air from entering the air intake system. If the test was with an actual automobile engine, combustion would have shut down long before the filter was completely occluded. It is expected that the actual time will be less for a larger system. After 124 seconds the pressure started to climb again because deformation of the filter occurred with continued vacuum, resulting in foam bypassing the filter. These tests confirm the effectiveness of the foam from disrupting the air flow required by internal combustion engines.

Conclusion

The ingestion of foam through the intake system demonstrates the overall effectiveness of this concept to meet the design objectives. The experiments that were conducted on an automobile intake system consisted of a shear stress experiment, foam flow, and discharge valve characteristics. The shear stress experiment determined that the stability of the foam would be adequate to be ingested into the air intake system, and the flow experimentation demonstrated the flow characteristics of the foam through the system. The discharge experiments found an optimum valve position to enable a reasonable discharge rate, foam volume, and pressure drop

for the discharge of foam. A half scale model was then developed to verify the foam characteristics and showed the viability of the system for the intended objective (stopping an automobile remotely).

CHAPTER 5 - Conclusions and Recommendations

Conclusions

The goal of the project was to develop a non-lethal system that can stop an automobile without damaging the vehicle or causing injury to the people inside. This goal was accomplished by developing a foam spray that can be discharged at a vehicle, engulfing the air intake system of the automobile, and disrupts combustion by occluding the pores of the air filter media. A literature review was conducted, and a starting point was outlined for work designed to optimize the surfactant composition, the discharge flow rate, and the absorption of carbon dioxide. Experimentation was completed on the variables of foam composition, absorption of carbon dioxide, and the discharge process of surfactant solution from a charged cylinder.

The primary variables of this project, identified by preliminary work, are foam composition, absorption of carbon dioxide, and an understanding of an automobile intake system. A literature review was conducted on the chemical components that could both improve foam characteristics, such as fluidity and stability, and on the rate of absorption of carbon dioxide. The literature review suggested that increasing the water concentration can increase the transient behavior of the foam, but adding solids, viscosifers, and surfactant solution could improve the stability of the foam. To improve the absorption of carbon dioxide alkoamines can be added to the surfactant solution. The literature review resulted in development of an initial composition of the surfactant solution for this project.

The literature review and the experimental work were used together to verify the behavior of the surfactant solution and to determine the optimum foam composition. The experiments consisted of bubble size distribution and foam interaction with filter medium. These two initial experiments checked the foams ability to work for this project.

The absorption of carbon dioxide was directly related to the volume of foam that could be generated and so an optimum method for the absorption had to be developed. Initially the absorption process was carried out by diffusion-limited mass transport of carbon dioxide, but this process was slow and resulted in an incomplete absorption process. The diffusion-limited absorption was modeled, and the model confirmed that carbon dioxide did not penetrate into the surfactant solution effectively. Therefore, the absorption process was changed to enhance the absorption process by promoting both convective and diffusive transport of carbon dioxide. This

resulted in a decreased absorption time with improved approach time to saturation. The model accurately predicted the experimental results for the rotating cylinder indicating that this method can be used for the absorption of carbon dioxide at a bench top scale.

The study of an automobile air intake system resulted in an initial experimentation to be developed. These tests include the ability to withstand shear stress generated by flow through the intake system and the foam's ability to flow through the system. It was found that the foam has enough stability to survive the air intake shear stress and can flow into the air intake system. These experiments led to additional experiments such as discharge velocity of foam being optimized and a model apparatus of the air intake being required. The secondary experiment on foam discharge found that the optimum discharge velocity of foam was 12.2-15.24 m/s. The model of the air intake system tested the foams ability to block the air flow of a half scale model and it was found that the foam would stop an automobile in less than six seconds. Even though it was found that the surfactant solution would stop automobiles, future research should be conducted to improve the final foam product.

Recommendations

The experiments determined that foam will stop an automobile, and the product will work for many military and police applications. Future research needs to be conducted on the effect of environmental conditions upon foam persistence and behavior, the stability of the product during long term storage, and improving the efficiency of foam expansion. In addition a full scale test is needed to verify the foam would stop an automobile. Laboratory testing of foam occurs at between 75 to 80 ºF with a relative humidity of about 50%, but it is unknown what impacts hot and dry conditions may have upon foam stability and deformability. The long term storage of the foam needs to be considered because it could be months before a hostile threat is encountered. Another important consideration is the need for improve efficiency when foam is being generated. The experimental trials were generating 60 to 65 liters of foam during the discharge, but ideally 378 liters of foam should be produced from the 682 grams of carbon dioxide that were absorbed. The inefficiency of the foam production means that currently the foam deployment apparatus, as developed for the laboratory, is about one order of magnitude too small to be practically useful. A commercial partner would then need to be identified as having the necessary resources and expertise to bring this work to the level of an actual field demonstration.

References

Adamson, A. W., & Gast, A. P. (1997). *Physical Chemistry of Surfaces.* United States: John Wiley and Sons inc.

Arntz, H. D., Otter, W. K., Briels, W. J., Bussmann, J. T., Beeftink, H. H., & Boom, R. M. (2008). Granular Mixing and Segregation in a Horizontal Rotating Drum: A Simulation Study on the Impactof Rotational Speed and Fill Level. *American Institute of Chemical Engineers , 54* (12), 3433-3146.

Bird, R. B., Stewart, E. W., & Lightfoot, E. N. (2002). *Transport Phenomena Second Edition.* John Wiley and Sons, INC.

Boateng, A. A., & Barr, P. V. (1997). Granular Flow Behavior in the Transverse Plane of a Partially Filled Rotating Cylinder. *Jounral Fluid Mechanics , 330*, 233-249.

Briceno, M. I., & Joseph, D. D. (2003). Self-Lubricated Transport of Aqueous Foams in Horizontal Conduits. *International jounral of Multiphase Flow , 29*, 1817-1831.

Carbon Dioxide Solubility in Water. (2003, June). Retrieved April 4, 2010, from http://www.kgs.ku.edu/PRS/publication/2003/ofr2003-33/P1-05.html

Dhanjal, S. K., Barr, P. V., & Watkinson, A. P. (2004). The Rotary Kiln: An Investigation of Bed Heat Transfer in Transverse Plane. *Metallurgical and materials Transactions, 35B*, 1059-1070.

Engineeringtoolbox.com. (2005). Retrieved April 4, 2010, from http://www.engineeringtoolbox.com/gases-solubility-water-d_1148.html

Farajzadeh, R., Barati, A., Delil, H. A., & Bruining, J. (2007). Mass Transfer of CO2 into Water and Surfactant Solutions. *Jouranl of Petroleum Science and technology , 25* (12), 1493-1511.

Gardiner, B. S., & Tordesillas, A. (2005). The Link Between Discrete and Continuous Modeling of Liquid Foam at the Level of a Single Bubble. *Journal of Rheolgy , 49* (4), 819-838.

Gautam, P. S., & Mohanty, K. K. (2004). Novel Aqueous Foams for Suppressing VOC Emission. *Environmental Science Technology , 38* (9), 2721-2728.

Gyenis, J. (1997, May 26-28). Segregation-Free Particle Mixing. *2nd Israel Conference for Conveying and Handling of Particular Solids* .

History of the Antique Fire Extinguisher. (1972). Retrieved 3 13, 2010, from http://www.historyoffirefighting.com/2008/11/antique-fire-extinguisher/

Janiaud, E., & Graner, F. (2005). Foam in a Two-Dimensional Couette Shear: a Local Measurement of Bubble Deformation. *Jounral Fluid Mechanics , 532*, 243-267.

Jonsson, B., Lindman, B., Holmberg, K., & Kronberg, B. (1998). Foaming of Surfactant Solutions. In *Surfactants and Polyymers in Aqueous Solution* (pp. 325-336). Baffins Lane, , England: John Wiley and Sons.

Jonsson, B., Lindman, B., Holmberg, K., & Kronberg, B. (1998). *Surfactants and Polymers in Aqueous Solutions.* New Yourk, NY: John Wiley and Sons.

Kato, A., Ibrahim, H., Watanabe, H., Honma, K., & Kobayashi, K. (1990). Enthalpy of Denaturation and Surface Functional Properties of Heated Egg White Proteins in the Dry State. *Journal Food Science , 55* (5), 1283-1295.

Komati, S., & Akkihebbal, S. K. (2008). CO2 Absorption into Amine Solutions: A novel Strategy for Intensifiction based on teh Addition of Ferrofluids. *Jounal of Chemical Technology and Biotechnology , 83*, 1094-1100.

Kundu, M., & Bandyopadhyay, S. S. (2006). Solubility of CO2 in Water+ Diethanolamine+ 2-Amino-2-methyl-1-propanol. *Jounral Chemical and Engineering Data , 51*, 398-405.

Lunkenheimer, K., & Malysa, K. (2003). A Simple Automated method of Quantitative Characterization of Foam Behaviour. *polymer International , 52*, 536-541.

National Fire Protection Association. (1972). *Fire-Fighting Foams and Foam Systems: A compliation of Article from Fire Jounral, Fire Command, and Fire Technology.*

Pratt, E., & Dennin, M. (2003). Nonlinear Stress and Fluctuation Dynamics of Sheared Disordered Wet Foam. *Physical Review , 67*.

Rocha, S. R., & Johnston, K. P. (2000). Interfacial Thermodynamics of Surfactants at the Cabon Dioxid-Water Interface. *Langmuir , 16* (8), 3690-3695.

Schilling, U., & Siekmann, J. (1982). Numerical Calculation of the Translational Forced Oscillations of a Sloshing Liquid in Axially Symmetrci Tanks. *Israel Journal of Technology , 20*, 201-205.

U.S Department of Energy. (n.d.). Retrieved May 25, 2010, from http://www.energy.gov/news/archives/6443.htm

Weihs, D., & Dodge, F. T. (1991). Liquid Motions in Nonaxisymmetric, Partially Filled Containers Rotating at Zero Gravity. *Journal Spacecraft , 28* (4), 425-432.

Wei-rong, Z., Hui-xiang, S., & Da-hui, W. (2004). Modeling of Mass Transfer Characteristics of Bubble Column Reactor with Surfactant Present. *Journal of Zhejiange University Science, 5* (6), 714-720.